IRON PNICTIDE SUPERCONDUCTORS

By

SHEWANGIZAW HAMELO

SUBMITTED IN PARTIAL FULFILLMENT OF THE
REQUIREMENTS FOR THE DEGREE OF
MASTER OF SCIENCE IN PHYSICS
AT
ADDIS ABABA UNIVERSITY
ADDIS ABABA, ETHIOPIA
JUNE 2011

ADDIS ABABA UNIVERSITY
DEPARTMENT OF
PHYSICS

Supervisor: _____

Examiners: _____

_____

ADDIS ABABA UNIVERSITY

Date: **June 2011**

Author: **SHEWANGIZAW HAMELO**

Title: **IRON PNICTIDE SUPERCONDUCTORS**

Department: **Physics**

Degree: **M.Sc.** Convocation: **June** Year: **2011**

Permission is herewith granted to Addis Ababa University to circulate and to have copied for non-commercial purposes, at its discretion, the above title upon the request of individuals or institutions.

Signature of Author

Table of Contents

List of Figures

Acknowledgements

Next to my God,I would like to thank my advisor Prof.P.Singh for his encouragement and valuable coments during writing up of this project paper.

Abstract

The discovery of new superconductor $LaFeAsO_{i-x}F_x$ with a superconducting critical temprature, T_c of 26K in 2008 has quickly renewed interest in the exploration of iron-based superconductors. More new superconductors have been discovered with the highest T_c of up to 55K being observed in the $SmFeAsO_{1-x}F_x$ compound. High T_c have previosly only been observed in cuprates, these new iron based superconductors have been added as second member of high T_c family. The crystal structur of these compound contains an almoost 2D Fe-As layer formed by $FeAS_4$ tetrahedrons,which can be separeted an ionic layer that provides an extra electron to Fe-As layer superconductivity can be induced by carrier doping,which destroy the antifrromagnetic ground state. The pairing mechanisim has been clarified as unconventional and antiferromagnetic(AF) spin fluctuations (SFs) seem to play an important role in making these pairs. In this paper superconducting crystal structur, physical properties of parent compounds, pressure effects, the electronic state of the compounds will be presented.

Introduction

Superconductivity is one of the most peculiar phenomena in nature. Its zero electrical resistance and fully repulsion of magnetic field (known as Meissner effect[1]) have great potential uses in practical applications. The first superconducting phenomenon was discovered in 1911 by Heike Kamerlingh Onnes, [2] who found that the resistance of solid mercury disappeared abruptly at 4.2 K. Since this discovery, scientists have been seeking superconductors with higher temperatures. In 1913, lead was found to superconduct below 7 K and in 1941 niobium nitride was found to superconduct at 16 K.

Since the first discovery of superconductivity in mercury in 1911, the underlying mechanism has been a major challenge to condensed matter physics community. In 1935, the brothers F. and H. London [3] explained the Meissner effect as a result of the minimization of the electromagnetic free energy carried by superconducting current. The famous London equations described the two basic electrodynamic properties mentioned above very well. In 1950, Landau and Ginzburg [4] developed the phenomenological Ginzburg-Landau theory by introducing a complex pseudowave function as an order parameter within Landaus general theory of second order phase transitions which led to a Schrodinger like wave function equation. The Ginzburg-Landau theory explained the macroscopic properties of superconductors successfully. By applying the Ginzburg-Laudau theory, Abrikosov [5] showed that superconductors could be grouped into Type I and Type II superconductors in 1957. Also in 1950, Maxwell and Reybold et al.[6, 7] found the isotope effect which showed that the critical temperature of a superconductor depends on the isotopic mass

of the constituent element. This important discovery pointed to the electron- phonon interaction as the microscopic mechanism responsible for superconductivity. The complete microscopic theory of superconductivity was finally proposed in 1957 by Bardeen Cooper and Schrieffer known as the BCS theory [8] In the BCS theory, they showed that pairs of electrons (known as Cooper pairs) could form through even a weak attractive interaction between electrons, such as electron-phonon interaction. The supercurrent is explained as a superfluid of Cooper pairs. The superconductivity phenomenon was explained independently in 1958 by Nikolay Bogoliubov [9] who was able to use a canonical transformation of the electronic Hamiltonian to derive the BCS wavefunction, which was obtained from a variational method in the original work of Bardeen, Cooper, and Schrieffer. In 1959, Lev Gorkov [10] showed that the Ginzburg-Laudau theory was a limiting form of the BCS theory close to the critical temperature. BCS theory is the most successful theory to explain superconductivity in conventional superconductors. Nevertheless, superconductivity in many superconductors remains unexplained,including high temperature superconductors (HTS, namely, the cuprates), the newly discovered iron-based superconductors, some organic superconductors and heavy fermion superconductors (eg: the 115 materials). The most wellknown superconductors are the cuprates,this first discovered by Bednorz and M ller[11] in 1986 in a lanthanum-based cuprate perovskite material with T_c of 35 K (Nobel Prize in Physics, 1987). It was shortly found by Wu et al.[12] that replacing the lanthanum with yttrium , i.e. making YBCO, raised T_c to 92 K. The highest T_c superconductor of this class (and among all superconductors) is the $HgBa_2Ca_2Cu_{38+x}$ compound under pressure with T_c about 160K. [13]

The other class is the iron-based superconductors, first discovered in February 2008 by Hosono et al [14] in a fluorine-doped tetragonal material $LaFeAsO_{1-x}F_x$ with T_c =26 K. Replacing the lanthanum in $LaFeAsO_{1-x}F_x$ with other rare earth elements such as cerium [15], praseodymium[16], neodymium [17], samarium [18,19], and gadolinium [20], increases T_c up to 56K.(the highest Tc in this class up to now) The figur.1 below shows

the time evolution of superconductors.

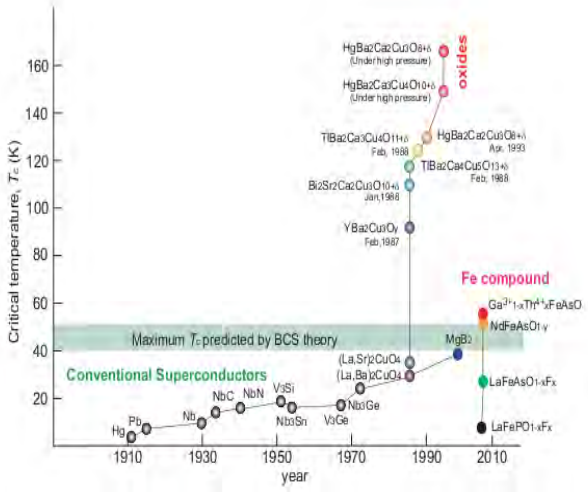

Figure 1: The time evolution of the superconducting critical temperature.

A few other (doped) materials were also found to superconduct at a relatively high temperature in the range of 10-40 K. A partial list of these materials [22] is doped C_{60} (T_c up to 40 K), $Ba_{1-x}K_xBiO_3$ (T_c up to 35 K), doped HfNCl (25 K) and ZrNCl (15 K), $Ba_2Nb_5O_x$ and $BaNbO_{3-x}$ (22 K), YPd_2B_2C (14 K), $PuCoGa_5$ (18 K). All of these material are structurally complex and are not phonon-mediated superconductors. The mechanism(s) responsible for their relatively high T_c superconductivity is (are) less known.

The simmering state of superconductor discovery has been re-ignited by discovery of a new class of layered transition metal pnictides ROTPn, where R is a trivalent rare earth ion, T is a transition metal ion, and Pn is a pnictogen atom. The breakthrough of T_c =26 K was reported [23] for 0.04 $\leq$ x $\leq$ 0.12 electron doped $LaFeAsO_{1-x}F_x$, followed by the demonstration that hole-doping [24] in $LaFeAsO_{1-x}Sr_x$, $0.09 \leq x \leq 0.20$, leads to a similar value of T_c . These values of T_c have now been superseded by the finding that replacement of La by Ce [25],Pr [26], Nd [27], Sm [28, 29] and Gd [30] result in $T_c = 41 - 55K$, substantially higher than in any materials except for the cuprate HTS.

Very soon, a few other Fe based compounds were found to be superconducting when doped or compressed. Currently, the parent compounds of Fe-based superconductors include

ZrCuSiAs-type RFeAsO and MFeAsF (1111-type), $ThCr_2Si_2$-typeMFe_2As_2(122-type), Cu_2Sb-type AFeAs (111-type), -PbO-type FeTe and FeSe (11- type), and $Fe_2As_2Sr_4X_2O_6$ (22426-type) (R=rare earth metal; M =Sr and Ca; M = Ba, Sr, Ca and Eu; A=Li and Na; X= Sc, Cr). [14, 15, 17, 20, 30, 31,32, 33, 34, 35, 36, 37]

In the vicinity of room temperature, these compounds crystallize in tetragonal symmetry with no magnetic order. The crystal structures of all the iron-pnictides share a common two-dimensional FePn layer, where Fe atoms form a 2D square sublattice with Pn atoms sit at the center of these square (figur1.2 below), but off the Fe plane (above and below the plane alternately). The FePn layer is different from the CuO layer in cuprates where the Cu and O atoms are in the same plane. The parent compounds of these iron-pnictides are metallic, while the parent compounds of cuprates are Mott insulators. At some lower temperature (which can be in the range of 100-210 K), they undergo a first or second order structural transition at T_S from tetragonal to orthorhombic, and magnetic transition at T_N from non-magnetic to stripe- antiferromagnetic.[38, 39, 40, 41] The structural transition and magnetic order transition can happen simultaneously or successively depending on the compound. It was confirmed both experimentally and theoretically that the magnetic order of Fe at low temperature is stripe-like antiferromagnetism often referred to as spin density wave (SDW). [38, 40, 41, 42, 43] Upon doping or compressing, the magnetic order goes away and the materials become superconducting. In the 1111-family (both RFeAsO and M FeAsF, R=rare earth and M =Ca and Sr), $T_N$is lower than T_S, which seems to suggest that the magnetic transition is induced by the structural transition. In the MFe_2As_2 (M =Ba, Sr, Ca, and Eu) compounds, $T_N = T_S$, i.e., the structural and magnetic transitions happen simultaneously (a first-order transition). Wheather the magnetic transition is induced by the structural transition or not and what is the driving force of the structural transition are two important questions that are crucial to understand the formation of the stripe antiferromagnetic order in the parent compounds.

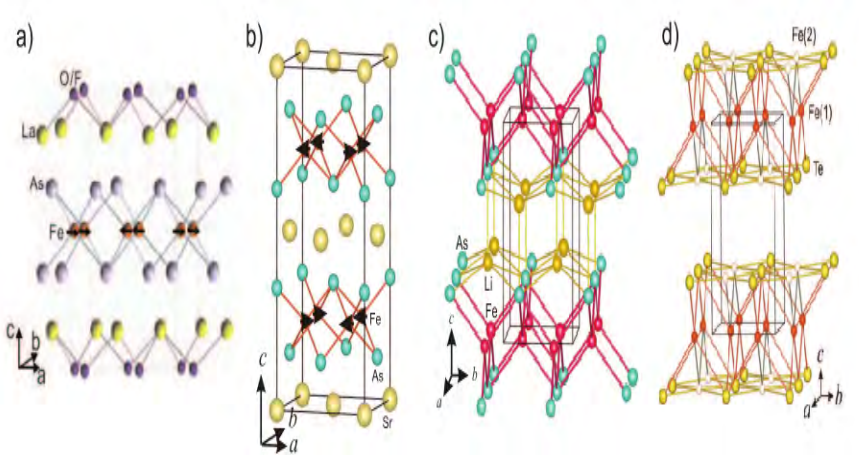

Figure 2: (Color online) Comparison of the crystal structures of (a) $LaFeAsO_{1-x}F_x$, (b) $SrFe_2As_2$, (c) LiFeAs, and (d) Fe_{1+x} Te. Each of these structures contains a square lattice of Fe atoms at high temperatures that can distort at low temperatures. Each Fe atom is tetrahedrally coordinated by As (a,b,c) or Te (d). In (b), the outline of the low-temperature orthorhombically distorted unit cell is shown, and ordered magnetic moments on the Fe atoms below the magnetic ordering temperature are shown by arrows. In (d), the Fe(2) atoms are the extra x atoms in $Fe_{1+x}Te$, .

Many experiments have been done to measure various properties of these iron- pnictide compounds. The ordered magnetic moment of iron is typically less than $1.0\mu B$, which is much smaller than the calculated value ($\sim 2.0\mu B$) from first principle calculations. The superconducting gap is best fitted to s± wave[287, 288] which is different from the dx^2–y^2 symmetry in cuprate superconductors. The oxygen-isotope effect is much smaller than the iron-isotope effect, which verifies the superconductivity comes from the FeP n layer. T_c is maximum when the $Fe-P-n-Fe$ angle ism about 109.4^o , suggesting that the height of the P n atom is very important to superconductivity. Superconductivity can be induced by different ways including electron doping, hole doping, vacancy and applying pressure. The phase diagram of the iron- based superconductors is similar to the cuprate superconductors.

Hundreds of theoretical papers have been published since the first report[14] in February, 2008. While much progress has been made on the understanding of these compounds, there are still fundamental questions which remain unanswered, such as:

- Itinerant vs. localized: Are the iron 3d electrons itinerant or localized?
- Driving force of phase transitions: What is the relation of the structural transition and the magnetic transition? What is the underlying driving force?
- Failure of L(S)DA and GGA: Since it has been confirmed from LDA+DMFT calculations[290] that LaFeAsO is a moderately correlated system, L(S)DA should work satisfactorily. Why L(S)DA fails to predict the correct position of As atom with an unacceptable large error of more than 0.1 ? Why LSDA and GGA overestimate A the ordered magnetic moment of iron in the stripe-AFM state by a huge amount?
- Pairing mechanism: What is the pairing mechanism of superconductivity in these compounds? Is it spin fluctuation, orbital fluctuation, electron-lattice interaction or something else?

Chapter 1

Overview of superconductivity

1.1 superconductvity

Superconductivity occurs when electrical resistivity of the specimen drops to zero when cooled to a sufficiently low temperature also know as critical (transition) temperature, T_C. Below T_C resistivity is zero, not just close to zero. This was, for instance, demonstrated by injecting

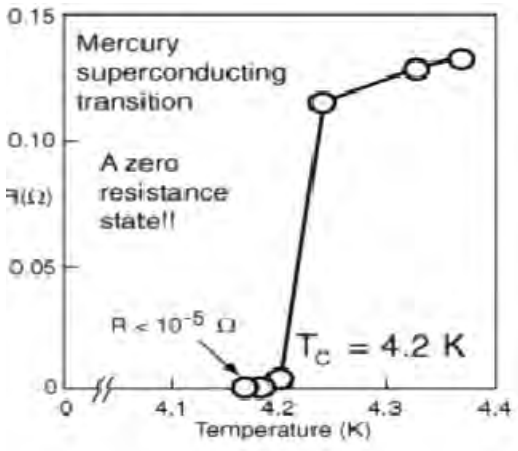

Figure 1.1: Resistance in ohms of a specimen of mercury versus absolute temperature by Kamerlingh Onnes in 1911 [1].

current into lead superconducting (SC) wire. This SC current persists almost indefinitely as long as $T < T_C$. In Figure 1.1 shows the historical electrical measurement of Kamerlingh Onnes, who first reported on a discovery of superconductivity in mercury in 1911.

Transition temperature for mercury is 4.2 K (Figure 1.1).

1.2 Meissner-Ochsenfeld effect

When the specimen is placed in a magnetic field, and then cooled, the magnetic flux is expelled from the specimen (Figure 1.2). This is known as Meissner effect. If there would be any magnetic field in superconductor it would change

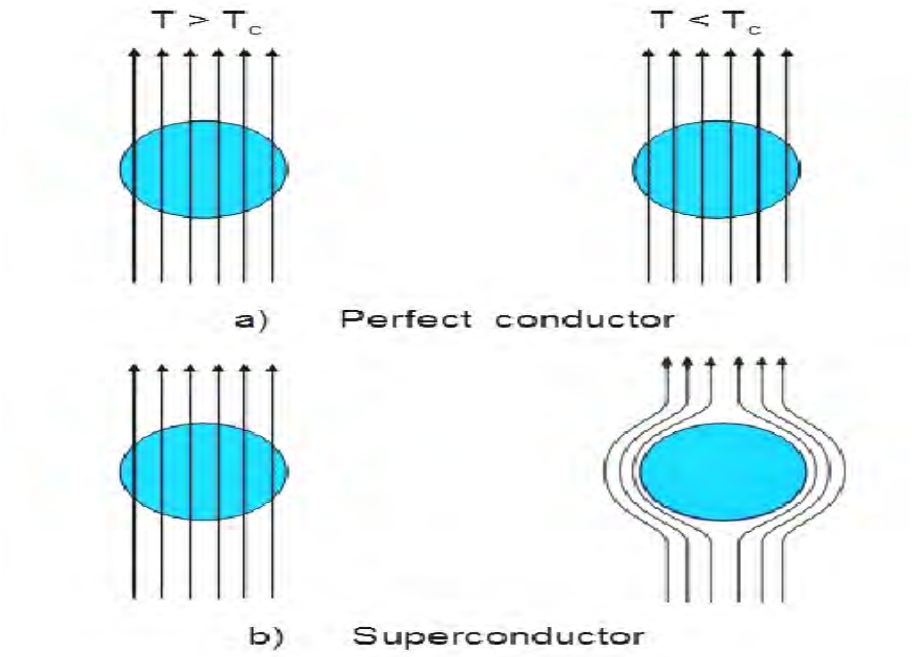

Figure 1.2: Meissner effect in a superconducting sphere, which is cooled in a constant applied magnetic field; below critical temperature the lines of induction B are ejected from the sphere (a) Perfect conductor, (b) Superconductor.

the flux. According to Lenz's law a current would be generated, which would oppose the flux, and eject any magnetic field from the superconductor. For the case, when magnetic field is expelled from the specimen, we can write

$$B = 0 = \mu_o(H + M) = \mu_o H(1 + \chi) \tag{1.2.1}$$

Here M is magnetization and χ, is magnetic susceptibility. Because there is no magnetic

field in specimen we can see from equation (1) that $\chi = -1$ A superconductor in magnetic field will act as a perfect diamagnet.

1.3 London equation describes Meissner effect

London equation can correctly predict magnetic field penetration into the SC material, but cannot give a microscopic picture. Let us assume a two-fluid model [4], where we distinguish between normal electrons and superconducting electrons $n = n_N + n_S$, where n is the electron density. As it was proved by the BCS theory, n_S are Cooper pairs, which are bound states of electron pairs. For superconducting electrons in electric field we can write

$$m\frac{\partial v_s}{\partial t} = -e_o E \tag{1.3.1}$$

If we consider equation for current density and apply it for superconducting electrons

$$j_s = -e_0 n_s v_s \tag{1.3.2}$$

$$\frac{\partial j_s}{\partial t} = \frac{n_s e_o^2}{m} E \tag{1.3.3}$$

Combining this with Faradays law $\bigtriangledown \times E = -\frac{\partial B}{\partial t}$ we obtain

$$\frac{\partial}{\partial t}(\bigtriangledown \times j_s + \frac{n_s s e_o^2}{m} B) = 0 \tag{1.3.4}$$

At this stage Fritz London took into account also the Meissners effect i.e. the magnetic field in superconductor is zero, and derived

$$\bigtriangledown \times j_s = -\frac{n_s e_0^2}{m} B. \tag{1.3.5}$$

If equation (1.3.5) is combined with $\bigtriangledown \times B = \mu_0 j_s$ we get

$$\bigtriangledown^2 B = \frac{\mu_0 n_s e_0^2}{m} B = \frac{1}{\lambda^2} B \Longrightarrow B(x) = B_0 \exp(-\frac{x}{\lambda}) \tag{1.3.6}$$

where $\lambda = \sqrt{\frac{mc^2}{4\pi n_s e^2}}$ is a London penetration depth, which measures the depth of penetration of the magnetic field. Inserting typical values for the density of SC charges for standard superconductors it is in order of 10 nm, while in HTSC it is around 100 nm.

1.4 Coherance length and penetration depth

Two characteristic lengths for superconductors can be defined qualitatively. One is ζ named as coherence length over which the order parameter ψ varies significantly and we will see later that the coherence length is the size of the Cooper pair in the microscopic theory.

$$\zeta = \sqrt{\frac{\hbar^2}{2m^*|a|}}$$

The other one is penetration depth λ, over which the magnetic field can penetrate into the surface appreciably,

$$\lambda = \sqrt{\frac{mc^2}{4\pi n_s e^2}} \tag{1.4.1}$$

It can be seen that the superfluid density $n_s \propto \lambda^{-2}$

1.5 Type I and type II superconductors

The superconducting state in specimen is destroyed if the specimen is placed in a sufficiently strong magnetic field (critical field, H_c) or if we generate strong enough currents (critical current $> 10^5 \frac{A}{cm^2}$) Based on this we distinguish two types of superconductors: type I and type II. Type I superconductor expels a magnetic field for $H < H_c$ while for $H > H_c$ superconductivity is destroyed and the field penetrates completely into the sample (Figure 1.3). A type II superconductor expels field in the normal state completely under H_{c1} . When H exceeds H_{c1} the field is only partially excluded, and the bulk specimen remains to be superconducting. Between $H_{c1} and H_{c2}$ the superconducting state

coexists with normal state regions where magnetic field penetrates into the sample.

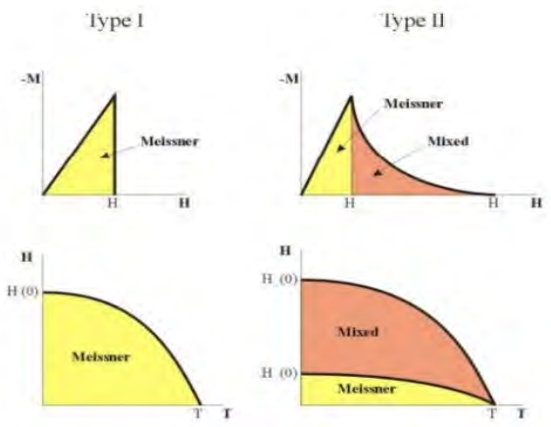

Figure 1.3: Magnetization properties of type I and type II superconductors.

1.6 Ginzburg-Landau theory and type II superconductor

Ginzburg-Landau theory is the most successful macroscopic theory to describe superconductivity [46, 47, 48]. Without knowing the microscopic mechanism, Ginzburg and Landau amazingly predicted the behavior of superconductors based on excellent physics intuition. Three assumptions were made. First, Landau second-order phase transition theory is applicable for superconductors since the phase transition from superconducting state to normal state is a second-order one when the external magnetic field is zero. Second, quantum mechanics should be reasonably combined into Landau theory since superconductivity is a quantum phenomenon rather than a classical one. It assumed all superconducting electrons behaved coherently and superconducting electrons could be described by a single phased wavefunction $\psi(r) =\mid \psi(r)e^{i\hat{\phi}t} \mid$. Third, $\psi(r)$ can be used as the order parameter.

For an inhomogeneous superconductor in a magnetic field, the Gibbs free energy can be

written as :

$$G_s(H) = G_n + \int \left(frac\hbar^2 2m^* |\nabla\psi - i\frac{e*}{\hbar c} A\psi|^2 + a|\psi|^2 + \frac{b}{2}|\psi|^4 + \frac{B^2}{8\pi} - \frac{B.H}{4\pi} \right) dV \right) \quad (1.6.1)$$

where A is the magnetic vector potential, the magnetic induction $B = \nabla \times A$, H is the external magnetic field, $\frac{B^2}{8\pi}$ is the magnetic field energy, $\psi(r) =\mid \psi(r)e^{i\hat{\phi}t} \mid$ is the order parameter which can be normalized so that $|\psi(r)|^2$ is equal to the superfluid density, $|\psi(r)|^2 = n_s^*$. $a(T) \approx a_o(\frac{T}{T_c} - 1), b(T) \approx b_o$

By minimizing the Gibbs free energy by $\frac{\partial G_s}{\partial \psi} = 0$ and $\frac{\partial G_s}{\partial A} = 0$ two coupled Ginzburg-Landau equations can be obtained. These two equations together with eq. 1.6.1 set up the basis of GL theory.

Chapter 2

BCS theory

In 1950, two groups independently found that different isotopes of mercury have different T_c [49, 50] which were later found to obey the relation $T_c M^{\beta}$= constant, where M is the mass of the isotope. Inspired by this isotope effect, Bardeen, Cooper and Schrieffer (BCS) assumed an electron-phonon interaction as the pairing mechanism Although other pairing mechanisms, like spin fluctuation, etc, were hypothesized for nonconventional superconductors, the idea of the formation of Cooper pairs, the key ingredient of superconductivity remains the same. In BCS theory, to simplify the calculation, a lot of assumptions were made, such as constant electron-phonon interaction, Fermi sphere assumption, etc,

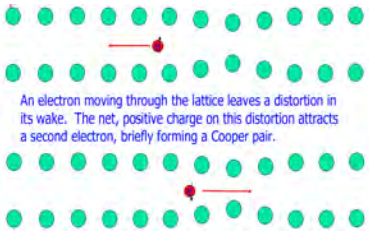

Figure 2.1: electron indirect interaction in crystal for pairing mechanisim.

2.1 Superconducting state

In 1950, Froholich [52] demonstrated that electrons can indirectly interact with each other in a crystal by emitting and absorbing phonons (fig 2.1). Electron 1 with wave vector k_1 emits a phonon and goes to state k_1, electron 2 with wave vector k_2 absorbs this phonon

and goes to state k_2 . This process can be understood as (k_1, k_2) state is scattered to (k_1, k_2) state by phonon. By this interaction, electrons within a thin shell of ω_D in the vicinity of the Fermi surface are attractive to each other.

In 1956, Cooper considered two electrons which are attractive to each other above the Fermi surface, he solved the two body Schrodinger equation and calculated the binding energy of these two electrons. He found the binding energy is always negative and a bound pair with negative potential can always be formed no matter how small the interaction is [53].

Combining the two facts above, Bardeen, Cooper and Schrieffer developed the microscopic theory of superconductivity. In a crystal, electron pairs in the ω_D shell near Fermi surface are formed due to the electron-phonon interaction and scattered from below the Fermi surface to above the Fermi surface, the potential energy is lowered while the kinetic energy is increased in this process. If the decrease of potential energy is larger than the increase of the kinetic energy, the ground state of the system is no longer the one for the normal state that all the electrons occupy the states inside the Fermi surface, as shown in (Fig. 2.2(a)), but rather the one in which some states above Fermi surface were occupied and some states below Fermi surface were empty, as shown in Fig. 2.2 (b). To form as many pairs as possible, so that the lowest energy can be achieved, the two electrons in one pair will be favored with opposite momentum,which mean $k_1 = -k_2 = k$, and if we also consider the electron spins, antiparallel configuration often lowers the energy even more. The electron pair with momentum $(k, -k)$ and antiparallel spin is called Cooper pair. Due to the Pauli exclusion principle, the wavefunction of the pair state should be antisymmetrical under the particle exchange.

If the spin of these two electrons form a spin singlet state (S=0), the spacial wavefunction should be with one even parity, which means the angular momentum should be L=0, 2, 4..., etc. If the spins form a spin triplet state (S=1), the spacial wavefunction should have odd parity and the angular momentum should be L=1, 3, ..., etc. In very rare

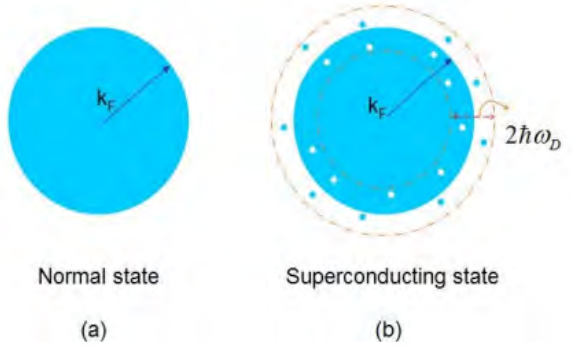

Figure 2.2: Schematic diagram of Fermi surface at (a) Normal ground state,(b) Superconducting state.

situations, such as ferromagnetic superconductorSr_2RuO_4 [54], Cooper pairs are thought to be formed with parallel spins.

In BCS theory, to simplify the calculation, several assumptions are made. First, the Fermi surface is assumed to be a sphere. Second, the pair state is assumed to be with L=0 and S = 0. Third, the electron-phonon interaction, $V_{kk'}$, is simplified as a constant:

$$V_{KK'} = \begin{cases} -V & if|\varepsilon_k|<\hbar\omega_D,|\varepsilon_{k'}|\leq\hbar\omega_D \\ O & if|\varepsilon_k|>\hbar\omega_D,|\varepsilon_{k'}|>\hbar\omega_D \end{cases} \tag{2.1.1}$$

where ε_k is the relative kinetic energy of the electron defined as

$$\varepsilon_k = \frac{\hbar^2 k^2}{2m} - \frac{\hbar^2 k_f}{2m} \tag{2.1.2}$$

The superconducting gap is a very important quantity in superconductors not only because it is closely related to the Cooper pair state and superconducting order parameter. It was proved [54] that the order parameter $\psi(r)$ in Ginzburg-Landau theory is actually the pair wavefunction in microscopic theory and is proportional to the superconducting energy gap. Therefore, by measuring the supercondcuting gap, information obout the pairing symmetry, which is critical in determining the pairing mechanism, can be provided. Fig. 2.3 shows the schematic representation of Δ in k space. Fig.2.3 (a) shows the isotropic s-wave superconducting gap with L = 0 and S = 0, the superconductor is fully

gapped, which is the situation discussed in the original BCS theory. For the so called s -wave pairing symmetry, which was proposed to be favored in FeAs based superconductors, the superconductor is fully gapped on both the electron and the hole Fermi sheets but with opposite signs between them [54,55,56,57,58] Fig. 2.3 (b) shows the anisotropic p- wave gap with L = 1 and S = 1. Fig. 2.3(c) and (d) show the anisotropic d- wave gap with L = 2 and S = 0

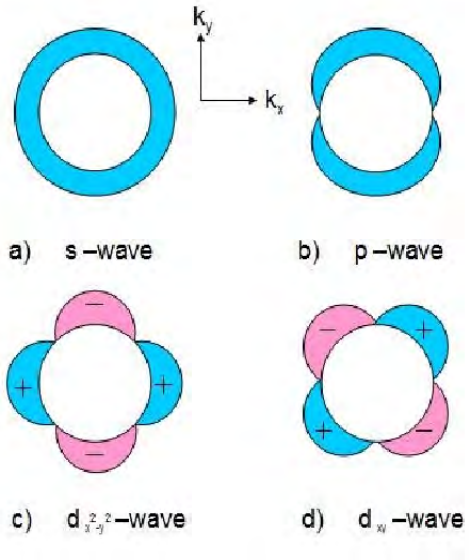

Figure 2.3: Superconducting gap with different gap in k space.

2.2 The gap equation and critical temperature

the hamlitonian $H = H_{KE} + H_v$, the single electron part is

$$H_{KE} = \sum_{k\sigma} \epsilon_k C^+_{\epsilon_k} C_{\epsilon_k} \tag{2.2.1}$$

where ϵ_k measured from chemical potential μ ,the spin index σ rans over $\downarrow, \uparrow$ some times we will asume spherical symetry with $\epsilon \approx \hbar v_F(k - k_F)$ and unbounded k , but only where specialy noted .

The general form of interaction potential is

$$H_v = H_V^{(0)} + H_V^{(1)} \tag{2.2.2}$$

brocken up according to whether the electrons being scattered are singlet or triplet spin state respectively .

$H^{(0)} = \sum_{pkk,} V_{kk,}^{0,p}(c_{k,+\frac{p}{2}}^{+}, \uparrow c_{-k+\frac{p}{2}}^{+}, \downarrow, c_{-k+\frac{p}{2}}, \uparrow)$

$V_{kk,}^{0,p} = -V_{kk,}^{0,p}$ ensures the singlet symetry.

2.3 Bogoliubov effective hamlitonian

For a pair with a non zero total momentum

$$< c_{-k+\frac{p}{2}}, \downarrow \ c_{k+\frac{p}{2}}, \uparrow >= 0$$

The energy is lowered when this is nonzero for only one choise of p at p=0 it has the lowest energy

$$< c_{-k\downarrow} \ c_{k\uparrow} > \neq 0 \tag{2.3.1}$$

The effective hamilitonian of pairing term of the potential defined at those with p=0

$$H^{pair} = \sum_{kk\cdot} V_{kk\cdot}^{(o)} c_{k,\uparrow}^{+} c_{-k,\downarrow}^{+} c_{-k\downarrow} c_{k\uparrow} \tag{2.3.2}$$

substituting eq.2.3.1 to eq 2.3.2

$$H^{pair} = \sum_{kk,} V_{kk,}^{(0)}(< c_{-k,\downarrow}, c_{k,\uparrow} >^{*} c_{-k\downarrow}, c_{k\uparrow} + < c_{-k\downarrow}, c_{k\uparrow} > c_{k,\uparrow}^{+}, c_{k,\downarrow}^{+} - constant) \tag{2.3.3}$$

droping the constant and define.

$$\Delta_k = -\sum_{kk,} V_{kk,}^{(0)} < c_{-k,\downarrow} \ c_{k,\uparrow} > \tag{2.3.4}$$

$$H^{pair} = -\sum_{kk,} (\Delta_k^{*} c_{-k\downarrow}, c_{k\uparrow} + \Delta_k c_{k,\uparrow}^{+} c_{-k,\downarrow}^{+}) \tag{2.3.5}$$

This doesn't conserve particle number two fermions can be created from nothing or anihilated.

2.4 Bogoliubov quasiparticle operators

The hamlitonian in to quadratic form

$$H_{Bogo} \equiv H_{KE} + H_{pair}^{eff} \tag{2.4.1}$$

This put in the form

$$H_{Bogo} = \sum_{k\sigma} E_k A_{K\sigma}^{+} A_{K\sigma} \tag{2.4.2}$$

the fermion oprators $A_{K\sigma}^{+}$ and $A_{K\sigma}$ creat and anhilate the " Bogoliubov quasi particle "they will be linear combination of the creation and anhilation oprators for real electrons

$$A_{k\downarrow} \equiv u_k c_{k\downarrow} + V_k c_{-K\uparrow}^{+} \tag{2.4.3}$$

$$A_{k\uparrow} \equiv u_k c_{k\uparrow} - v_k c_{-k\downarrow}^{+} \tag{2.4.4}$$

while the creation oprators are conjugates of these

The quasiparticle number oprator

$$n^{pq} \equiv A_{k\sigma}^{+} A_{k\sigma} \tag{2.4.5}$$

each quasiparticle operator carries a defnite wave vector and spin. Thus in A_k^{+}, one oprator $(c_{k\uparrow}^{+})$ creates and electron an other oprator $(c_{-k\downarrow})$ creates a hole with the same quantum number $(k, \uparrow)$

$\Longrightarrow$ what are the nesesary condition for$\{A_{k\sigma}^{+}\}$ and $\{A_{K\sigma}\}$

to have canonical fermion transformation? the self -anticomutation gives a normalization condition

$$1 = \{A_{k\uparrow}^{+}, A_{K\uparrow}\} = \{u_k^{*} c_{k\uparrow}^{+} - v_k^{*} c_{-k\downarrow}, u_k c_{k\uparrow} - v_k c_{-k\downarrow}^{+}\} = u_k^2 + v_k^2 \tag{2.4.6}$$

otherwise anticomutators of bogoliubov oprators must give zero

$$0 = \{A_{k\uparrow}^{+}, A_{-K\downarrow}\} = \{u_k c_{k\uparrow} - v_k c_{-k\downarrow}^{+}, u_{-k} c_{-k\downarrow} + v_{-k} c_{k\uparrow}^{+}\} = u_k v_{-k} - v_k u_{-k} \tag{2.4.7}$$

this is satsfied if and only if we require $v_K = v_{-k}$

The inverse transformation reads

$$c_{k\uparrow} = u_k^* A_{k\uparrow} + v_k^* A_{-k\downarrow}^+ \tag{2.4.8}$$

$$c_{k\downarrow} = u_k^* A_{k\downarrow} - v_k^* A_{-k\uparrow}^+ \tag{2.4.9}$$

taking $u_k^* = u_k$ by convention

2.5 Bogoliubov cofficients and BCS wave functions

To solve the effciently u_k and v_k we substitute eq.2.4.3 and 2.4.4 to eq 2.4.2

$$\begin{aligned} H_{Bog} &= \sum_{k\sigma} E_K(u_k^* c_{k\uparrow}^+ - v_k^* c_{-k\downarrow}^*)(u_k c_{k\uparrow} - v_k c_{-K\downarrow}^+) \\ &= \sum_{k\sigma} E_k(u_k^* u_K(c_{k\uparrow}^+ c_{k\uparrow}) - u_k^* v_k(c_{k\uparrow}^+ c_{-k\uparrow}^+) - v_k^* u_k(c_{-k\downarrow} c_{k\uparrow}) + v_k^* v_k(c_{-k\downarrow} c_{-k\downarrow}^+) \\ &= \sum_{k\sigma} E_k[u_k^2(c_{k\uparrow}^+ c_{k\uparrow}) - |v_k|^2(c_{k\uparrow} c_{k\uparrow})] \end{aligned} \tag{2.5.1}$$

from equation 2.4.2 $H_{Bogo} = H_{KE} + H_{pair}^{eff}$ and 2.4.2 $H_{KE} = \sum_{k\sigma} \epsilon_k c_{k\sigma}^+ c_{k\sigma}$,

$$= \sum_{k\sigma} E_k[u_k^2(c_{k\uparrow}^+ c_{k\uparrow}) - |v_k|^2(c_{k\uparrow} c_{k\uparrow})] = \sum_{k\sigma} \epsilon_k c_{k\sigma}^+ c_{k\sigma}$$

$$E_k(u_k^2 - |v_k|^2) = \epsilon_k \tag{2.5.2}$$

and taking

$-u_k^* v_k(c_{k\uparrow}^+ c_{-k\uparrow}^+) - v_k^* u_k(c_{-k\downarrow} c_{k\uparrow})$ one can get

$$\begin{aligned} &\sum_{k\sigma} E_k[-u_k^* v_k(c_{k\uparrow}^+ c_{-k\uparrow}^+) - v_k^* u_k(c_{-k\downarrow} c_{k\uparrow})] \\ &= -\sum_k [\Delta_k^*(c_{-k\downarrow} c_{k\uparrow}) + \Delta_k c_{k\uparrow}^+ c_{-k\downarrow}^+] \\ &\sum_{k\sigma} E_k[u_k^* v_k(c_{k\uparrow}^+ c_{-k\uparrow}^+) + v_k^* u_k(c_{-k\downarrow} c_{k\uparrow})] = \sum_k [\Delta_k^*(c_{-k\downarrow} c_{k\uparrow}) + \Delta_k c_{k\uparrow}^+ c_{-k\downarrow}^+] \end{aligned}$$

$$2u_k v_k = \frac{\Delta_K}{E_k} \tag{2.5.3}$$

adding the the absolute square of eq(2.5.2)and eq(2.5.3)

$$\begin{aligned} 4u_k^2 v_k^2 &= \frac{\Delta_k^2}{E_k^2} \\ (u_k^2 - |v_k^2|)^2 &= \frac{\epsilon_k^2}{E_k^2} \\ (u_k^2 + |v_k^2)^2 &= \frac{\Delta_k^2 + \epsilon_k^2}{E_k^2} \\ E_k^2 &= \Delta_k^2 + \epsilon_k^2 \\ E_k &= \sqrt{\Delta_k^2 + \epsilon_k^2} \end{aligned} \tag{2.5.4}$$

where $u_k^2 + |v_k^2| = 1$ combining eq(2.5.2) and eq(2.5.4) gives the second big result the magnituyde of the coffcient themselves

$$u_k^2 = \frac{1}{2}\left(1 - \frac{\epsilon_k}{E_k}\right) \tag{2.5.5}$$

$$v_k = \frac{1}{2}\left(1 + \frac{\epsilon_k}{E_k}\right) \tag{2.5.6}$$

The quantity Δ_k is known as the gap function becouse it is most obvios effect is the gap A_{kF} in bogoliubov spectrum, but it is actualy a function defined for K far away from the the fermi surface.It is the centeral objective in BCS theory as E_K and the coffcient u_k and v_k that enters all physical expectations depend on Δ_k.In this section we will obtain the self consistent equation for Δ_k and see how the Bogoliubov approach extends $T > 0$ Solving for Δ_k and evaluating $< c_{-k\downarrow} c_{k\uparrow} >$and converting electron to the quasi particle oprator

$$\begin{aligned} c_{k\uparrow} &= u_k^* A_{k\uparrow} + v_k^* A_{-k\downarrow}^+ \\ c_{k\downarrow} &= u_k^* A_{k\downarrow} - v_K^* A_{-k\uparrow}^+ \end{aligned} \tag{2.5.7}$$

where $u_k^* = u$ by convention

From eq (2.3.4)

$$\Delta_k = -\sum_k V^{(0)}_{kk,} < c_{-k,\downarrow} c_{k,\uparrow} >$$

$$\Delta_k = -\sum_k V_{kk,} < (u^*_k A_{k\downarrow} - v_k A^+_{-k\uparrow})(u^*_k A_{K\uparrow} + v^*_k A^+_{-k\downarrow}) > \tag{2.5.8}$$

$$\tag{2.5.9}$$

where A^+A^+ and AA are zero expectation

then we get

$$< c_{-k\downarrow} c_{k\uparrow} >= u_k v_k \Big(< A_{-k\downarrow} A^+_{-k\downarrow} > - < A^+_{k\uparrow} A_{k\uparrow} > \Big) \tag{2.5.10}$$

using

$2u_k v_k = \frac{\Delta_K}{E_k}$ and quasi particle number oprator eq. (2.4.5)

$$< c_{-k\downarrow} c_{k\uparrow} >= \frac{1}{2}\left(\frac{\Delta_k}{E_k}\right)\Big[1 - < n^{pq}_{k\uparrow} > - < n^{pq}_{k\uparrow} > \Big] \tag{2.5.11}$$

at T=0 we have $< n^{pq}_{k\uparrow} > \equiv 0$ so wesubstituting to eq.(2.3.4)

$$\Delta_k = -\sum_k V^{(0)}_{kk,} < c_{-k,\downarrow} c_{k,\uparrow} >$$

$$\Delta_k = -\sum_k \frac{V^{(0)}_{kk,}}{2}\left(\frac{\Delta_k}{E_k}\right)\Big[1 - < n^{pq}_{k\uparrow} > - < n^{pq}_{k\uparrow} > \Big]$$

$$\Delta_k = -\sum_k \frac{V^{(0)}_{kk,}}{2}\left(\frac{\Delta_k}{E_k}\right)$$

$$\Delta_k = -\sum_k \frac{V^{(0)}_{kk,}}{2}\frac{\Delta_k}{\sqrt{\epsilon^2_k + |\Delta_k|^2}} \tag{2.5.12}$$

where $E_k = \sqrt{\epsilon^2_k + |\Delta_k|^2}$

The trival solution Δ_k corresponds to the normal fermi gas and expecting nontrival solution with lower energy for atractive interaction

$$V(k,k') = \begin{cases} -V_O if |\epsilon_k| and |\epsilon_k| \leq \hbar\omega_c \\ 0 otherwise \end{cases} \tag{2.5.13}$$

where ω_c is the cut of frequency,the solution of the gap equation at T=0 is

$$\Delta_k = \begin{cases} \Delta_o for |\epsilon_k| and |\epsilon_k^{,}| < \hbar\omega_c \\ 0 for |\epsilon_k| > \hbar\omega_c \end{cases} \tag{2.5.14}$$

from eq(2.5.12) Δ_o satsfies

$$1 = \sum_{k,} \frac{V_0}{2\sqrt{\epsilon_k^2 + |\Delta_k|^2}} \tag{2.5.15}$$

and $\sum_k$ indicates that the summation is over K that satsfies $|\epsilon| < \hbar\omega_c$, Here the overall phase of Δ_o is such real and posetive ,changing the summation in to an integration we obtain.

$$\frac{1}{V_o} = \int_{\hbar\omega_c}^{\hbar\omega_c} d\epsilon \frac{N(o)}{\sqrt{\epsilon_k^2 + |\Delta_k|^2}} \tag{2.5.16}$$

where $N(\epsilon)$ is the density of states for electrons of one spin orientation. assuming $N(\epsilon)$ is slowly varing over the range of $|\epsilon| < \hbar\omega_c$

$$\frac{1}{N(O)V} = \int_0^{\hbar\omega_c} d\epsilon \frac{1}{\sqrt{\epsilon^2 + \Delta_o^2}} \tag{2.5.17}$$

integrating this we obtain

$$\frac{1}{N(o)V} = \ln \frac{\hbar\omega_c + \sqrt{(\hbar\omega_c)^2 + \Delta_o^2}}{\Delta_o} \tag{2.5.18}$$

This become

$$\Delta \approx 2\hbar\omega_c exp[-\frac{1}{N(o)V_o}] \tag{2.5.19}$$

The same grand result for BCS gap formula but with the correct prefactor

$$\Delta = \frac{\hbar\omega_c}{sinh(\frac{1}{N(o)V_o)}} \approx 2\hbar\omega_c exp[-\frac{1}{N(o)V_o}] \tag{2.5.20}$$

the exponential result only in the weak coupling regime.

The quantum expectations appearing in the decoupling (which were taken with respect to the ground state of the particle) to the thermal exapnsions,for an enesemble in which quasi particle state are occupied as independent fermions. At finite thempratur the expectation value of the quasi-particle number oprator in eq.(2.4.5)

$$< n_{k\sigma}^{pq} >_T = f_T(E_k) = \frac{1}{1 + e^{\frac{\beta E_k}{T}}} \tag{2.5.21}$$

where$\beta = \frac{1}{K_B T}$ and the chemical potential μ of quasi particle equal to zero.
The new gap equation looks like $\Delta_k = -\frac{1}{2}\sum_k V_{kk'}^{(o)} \frac{\Delta_k}{\sqrt{|\epsilon_k|^2+|\Delta_K|^2}}$ exept that a factor $tanh(\frac{E_k}{2T})$ inserted in the right hind side

$$\frac{1}{V_o} = \frac{1}{2}\sum_k \frac{tanh(\frac{\beta E_k}{2})}{E_k} \tag{2.5.22}$$

$\Longrightarrow$ As we rise T the tanh factor graduly takes over the job of suppresing the logarithimic divergence which was hndled by Δ in $E_k = \sqrt{\epsilon_k^2 + |\Delta_k|^2}$ in the denominator correspondingly the value of Δ will decrease.

$$\frac{1}{V_o} = \frac{1}{2}\sum_k \frac{tanh(\frac{\beta E_k}{2})}{E_K}$$
$$\frac{1}{V_o} = \int_0^{\hbar\omega_C} d\epsilon \frac{tanh(\frac{\beta}{2}\sqrt{\epsilon_k^2+\Delta^2})}{\sqrt{\epsilon_k^2+\Delta^2}}$$

The critical tempratur T_c determined by setting $\Delta(T) \to 0$

$$\frac{1}{N(0)V_o} = \int_0^{\beta_c\hbar\omega_c} dx \frac{tanhx}{x}$$
$$\frac{1}{N(0)V_o} = tanhx \ln x\Big|_0^{\beta_c\hbar\omega_c} - \int_0^{\beta_c\hbar\omega_c} sec^2 hx \ln x dx$$
$$\frac{1}{N(0)V_o} = \ln\left(\frac{2\gamma\beta\hbar\omega_c}{\pi}\right) \tag{2.5.23}$$

Where $\ln\gamma$ is Euler's constant equal to 0.577.. thus T is reduced, a critical tempratur T_c is reached given by

$$K_B T_c = \beta^{-1} = 1.14\hbar\omega_c exp[-\frac{1}{N(o)V_o}] \tag{2.5.24}$$

The above equation depends on three material properties

- The Debeye frequency ω_c
- V_0 measures the strength of electron-phonon coupling and
- N(o) that measures the number of electrons available at the fermi energy. Note that d-levels generally have higher $N(\epsilon_F)$ than p-levels or s- levels.

Chapter 3

High-Tc superconductivity in iron pnictides

High T_c superconductivity at 26 K was reported by Kamihara et al. in F-doped LaFeAsO [55] that appeared online on 23^{rd} of February 2008. This was the discovery of high T_c superconductivity in a completely new class of materials that came to be known as iron pnictides. This new discovery has generated a great interest in the materials science community opening a new route for the high T_c research in additon to that of the cuprates. However, this has also brought new challenges on both experimental and theoretical sides and added a new problem for material scientists in addition to the long standing problem of cuprates.

3.1 Different families of pnictides

▶ 1111 family : Following the discovery of high T_c superconductivity in $LaFeAsO_{1-x}F_x$, T_c rapidly increased by exchanging lanthanum with rare earth ions of smaller atomic radii in LnFeAsO and appropriate carrier doping or creating oxygen deficiencies, until it reached a maximum value of$\sim 56K$ until now in $Gd_{1x}Th_xFeAsO$ [56]. This family LnFeAsO came to be known as 1111 family. Note that LaFePO, also discovered by Kamihara et al. in 2006, was the first 1111 compound to show superconductivity, but with very low T_c ($\sim 5-7K$). In addition to $LaFeAsO_{1-x}F_x$, the most remarkable 1111 compounds that

show high T_c superconductivity discovered until now are: (i) $SmFeAsO_{1x}F_x$ ($T_c \approx 43K$) [57], (ii) $CeFeAsO_{1x}F_x$ ($T_c \approx 41K$) [58], (iii) $NdFeAsO_{1x}F_x$ ($T_c \approx 51K$) [59], and (iv) $PrFeAsO_{1x}F_x$($T_c \approx 52K$) [60].

► 122 family: M. Rotter et al. [61] proposed $BaFe_2As_2$ as a potential new parent com pound based on the similarities between $BaFe_2As_2$ and LaFeAsO. In fact, both compounds contain identical (FeAs) layers, and have the same charge accordance as follows: $Ba^{2+}[(FeAs)]_2 vs.(LaO)^+(FeAs)$. Partial replacement of Barium with Potassium (hole doping) induced superconductivity at 38 K in $Ba_{0.6}K_{0.4}Fe_2As_2$ [62], the first member of a new family of superconducting iron arsenides known as the 122 family. This discovery was followed by reports of similar compounds with: (i) strontium ($T_c \approx 37K$) [63, 64], (ii) calcium ($T_c \approx 20K$) [65], and (iii) europium ($T_c \approx 32K$). Later electron doping in $BaFe_2As_2$ by the partial replacement of Fe with Co with $T_c \approx 22K$ was reported by Sefat et al. [67].

► 111 famliy X. C. Wang et al. [68] reported the discovery of another new superconducting iron arsenide system LiFeAs (termed 111). Superconductivity with T_c up to 18 K was found in these compounds.

► 11 family F.-C. Hsu et al. [69] reported the observation of superconductivity with zero resistance transition temperature at 8 K in the PbO-type αFeSe compound known as 11 family. Although FeSe has been studied quite extensively, a key observation is that the clean superconducting phase exists only in those samples prepared with intentional Se deficiency.

3.2 Crystal structure and physical properties

The crystal structures of the four families of iron pnictides are discussed briefly below:

► 1111 family

LaFeAsO and the 1111 family of iron pnictides crystallizes in the ZrCuSiAs type structure, (space group ($p\frac{4}{nmm}$). In this structure, two dimensional layers of edge-sharing $FeAs_{4/4}$ tetrahedra alternate with sheets of edgesharing $LaO_{4/4}$ tetrahedra. Because of the differences between the ionic nature of the Ln-O (Lanthanum oxide) bonds and the more covalent Fe-As (iron arsenide) bonds, a distinctive

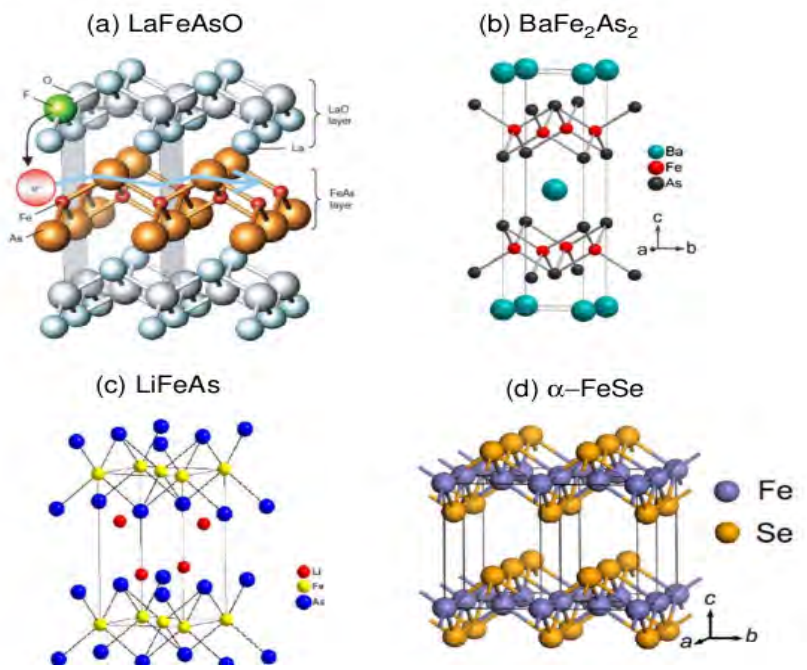

Figure 3.1: Schematic crystal structure of: (a) LaFeAsO [68], (b) $BaFe_2As_2$ [62] (c) LiFeAs [68] (d) FeSe [69]..

two-dimensional structure forms, where ionic layers of lanthanum oxide $(LaO)^+$ alternate with metallic layers of iron arsenide $(FeAs)^-$.

► 122 family

The ternary iron arsenide $BaFe_2As_2$, with the tetragonal $ThCr_2Si_2$ -type structure space group (space group I4/nmm) contains practically identical layers of edge-sharing $FeAs_{4/4}$ tetrahedra, but they are separated by barium atoms instead of LaO sheets. This structure is shown in Fig. 3.1 (b) [62].

► 111 family

LiFeAs crystallizes into a Cu_2Sb-type tetragonal structure containing [FeAs] layer with

an average iron valence Fe^{2+} like those for 1111 or 122 parent compounds. This structure is shown in Fig. 3.1 (c) [68].

3.3 Resistivity of iron pnictides

Parent compounds of iron pnictides show an anomaly in the resistivity curves at certain temperature that depends on the compound itself. Later, it was found out that this anomaly is due to a structural phase transition. Typical examples of resistivity curves of $LaFeAsO_{1x}F_x$ [19] and $BaFe_2As_2$ [26] are shown in panels a and b of Fig. 3.2

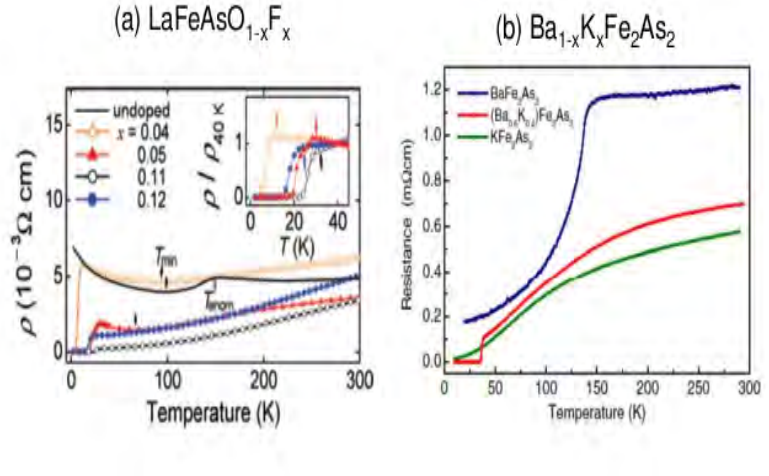

Figure 3.2: Typical resistivity curves of (a) $LaFeAsO_{1x}F_x$ [19] and (b) $(Ba, K)Fe_2As_2$ [62]. .

3.4 Factors affecting Tc in pnictides

It has been known that electron doping in the 1111 system can be done by substitution of oxide for fluoride or by oxide vacancies.

- Effect of Rare-earth elements

Rare earths with smaller ionic radii decreased the latice constant there by developing inner chemical pressure leading to high T_c Doping brings structural modification such as a reduction in cell volume decrease between layers and increase in distance between Re^{3+} and F^- which inhances spin and charge density fluctuation. As mentioned above, exchanging lanthanum with rare earth ions of smaller atomic radii in $LnFeAsO_{1-y}$, T_c was found to increase. This effect is summarized in Fig. 3.3 taken from Ref. [72].T_c increases from 28 K (Ln=La) to 53 K (Ln=Nd). However, T_c stays almost constant from Ln=Nd to Dy and this effect is not completely understood yet.

- Effect of pressure

Pressure inhancement increases charge transfer between the insulating LaO layer and the conducting FeAs layer, in addition the external pressure induces an anistropic shirinkage, which concidered as the main reason for further increase in onset T_c. It was found that pressure has a large effect on iron pnictides so that some parent compounds can become superconducting by simply applying pressure. As an example of the pressure effect, we remark that the T_c of the original system $LaFeAsO_{1x}F_x$ went up from $\sim 26K$ to $\sim 43K$ by applying a pressure of $\sim$ 4GPa [37].

- Effect of oxygen deficiency

Oxygen deficiency produces more latice shirinkage and charge carrier there by increase the density of state (DOS). T_c increase abrouptly to a maximum with a slight doping of oxygen vacancies and then decreased with further increase in oxygen vacancies.

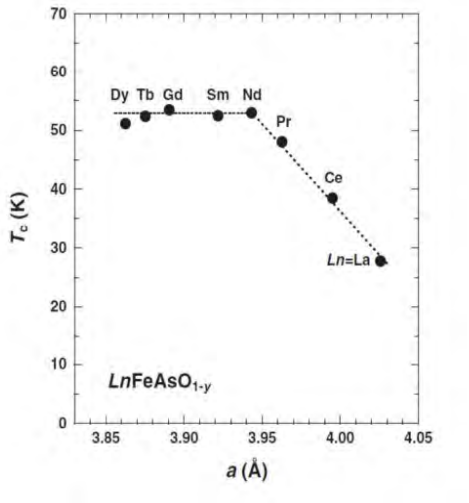

Figure 3.3: Ln-dependence of T_c for $LnFeAsO_{1y}$ system (Ln=La, Ce, Pr, Nd, Sm, Gd, Tb, and Dy). T_c is plotted against the a-axis lattice parameter [72].

3.5 Phase Diagrams

$\Rightarrow$ 1111 materials

The first evidence for the importance of magnetism in the Fe-based superconductors was the concentration dependent phase diagram presented with the initial discovery of superconductivity in F doped LaFeAsO [73]. An additional phase was clearly present at low F concentration which vanished at doping levels where superconductivity appears although the exact nature of this phase was unclear. It was soon shown that the undoped LaFeAsO parent compound exhibited spin-density wave (SDW) order below about 150 K [74, 75] . Unexpectedly, LaFeAsO also exhibited a structural phase transition [74] at a temperature slightly above the magnetic ordering temperature.

There is clear competition between magnetism and superconductivity as the magnetically ordered state is destroyed in the fluorine doped,superconducting samples [74, 75]. The phase diagram of $RFeAsO_{1x}F_x$ as a function of doping has been carefully studied for R = La [76] (figure 3.4(a)), Ce [77] (figure 3.4(b)), Pr [78] and Sm [79, 80] (figure 3.4(c)). The phase diagrams were experimentally determined using the following techniques: R = La, SR, 57 Fe Messbauer spectroscopy and x-ray diffraction [76]; R = Ce, neutron diffraction,

resistivity and magnetization [77]; R = Pr, x-ray diffraction, resistivity and magnetization [78]; R = Sm, typical structural transition at 150 K and SDW ordering at about 140 K. In general, doping causes a suppression of both the structural and magnetic phase transitions and as these are suppressed, superconductivity emerges. The fundamental difference between materials with different rare earths comes in the behavior near the emergence of superconductivity. For R = La and Pr, the structural and magnetic transitions in an abrupt step-like manner as a function of doping at the onset of superconductivity [76, 78], as shown in figure 3.4(a) for the case of R = La. For the case of R = Ce, the magnetic transition appears to vanish continuously to very low temperatures and superconductivity emerges at a concentration where this transition has been completely suppressed [77] (see figure 3.4(b)). However, the structural transition has some range of concentrations where superconductivity coexists with phase transition [77]. Finally, the case or R = Sm, shown in figure 3.4(c), looks similar to R = Ce in that the transitions are suppressed gradually and there appears to be overlap between the structural transition and superconductivity [80]. However, unlike the case of Ce, the Sm phase diagram shows a region where magnetic ordering coexists with superconductivity [79].

The above fig (d) the parent compound $BaFe_2As_2$ contains hole doping (K) and electron doping (Co)on FeAs plane.As the case of the 1111 parent compounds,122 exhibits both structural and phase transition from room temperatur $\frac{I_4}{mmm}$ space group to the low temprature to the low temprature ortorhombic Fmmn space group and magnetic trasition to a long range order SDW state. Unlike 1111 material both structural magnetic phase transition occour at the same temprature in 122 parent compound.In electron doping case and hole doping superconductivity emerges as the SDW order is suppresed.Interestingily in both case K and Co doping there is a region of phase diagram where the SDW state and structural transition coexist with superconductivity. This certainly shows a very strong interaction between the superconducting and SDW state. It could be interpreted that this suppression is due to the same electrons partcipating in both SDW and superconductivity

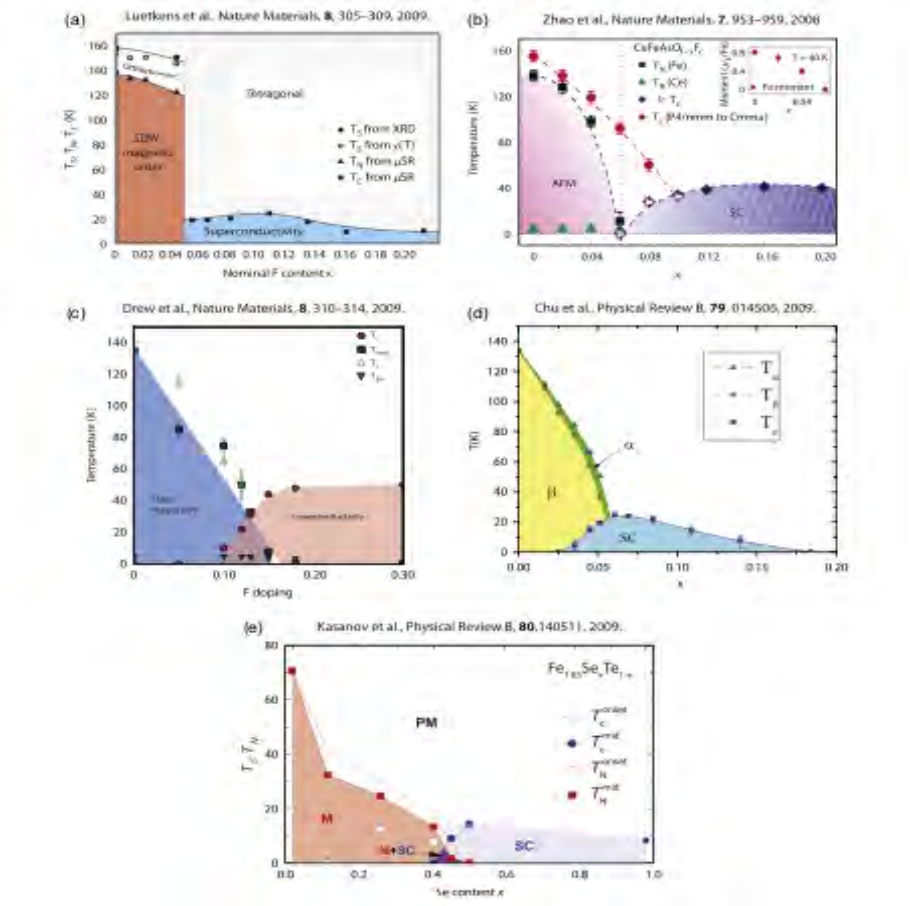

Figure 3.4: Experimentally determined phase diagram for (a) $LaFeAsO_{1x}F_x$ [76], (b) $CeFeAsO_{1x}F_x$ [77], (c) $SmFeAsO_{1x}F_x$, (d)$BaFe_{2x}Co_xAs_2$), and (e) $Fe_{1.03}Te_{1x}Se_x$.

in phase coexistance.

3.6 Electronic states

Comparing the 1111 and 122 ferropnictide compounds with each other, it becomes obvious that they have certain aspects in common. For example, their carriers are sharply localized in the planes perpendicular to the c-direction, making the material extremely anisotropic which means that they are, almost 2-dimensional with interlayer coupling in both the normal and the superconducting state. This is the case for all high-temperature superconductors. In the case of FeAs based superconductors, the electronic activities take

place in the square FeAs planes. The interlayer planes are purely ionic; their sole purpose is to act as dopant reservoirs. Superconductivity is a manifestation of quantum mechanics on a macroscopic scale. It is important to find whether the superconductivity in the new class of Fe based superconductors is conventional or unconventional like in the cuprates or have an entirely new mechanism. In conventional superconductors, it has been well established that electrons form so called cooper pairs to give rise to the superconductivity. The pair binding manifests itself as an energy gap in many spectroscopic measurements, the energy gap known as superconducting gap, appears at the transition temperature T_c where the resistance also vanishes. For high temperature superconductors this is more complicated since over the wide region of compositions and temperatures this energy gap exists quite well above the transition temperature . This is why this gap is called pseudo gap. The origin of pseudogap and the relation with the superconducting gap is believed to be the key to understand the mechanism of high temperature superconductivity.

All the conventional superconductors are well understood within the BCS theory as phonon mediated pairing of electrons and condensation of the resulting bosonic gas. All superconductors that can be understood within this theory have a transition temperature less than 40K. Preliminary experimental results such as specific heat (81), NMR spectroscopy (82) and high field resistivity measurement suggest the existence of unconventional superconductivity in these Fe based superconductors. It is pointed out in some papers (83, 84) that there is an essential similarity of electronic states near the Fermi level in 122 and 1111 family. Both families have been studied in many details by DFT (density functional theory) calculation. DFT is the quantum mechanical theory used in physics to investigate the electronic structure of many body systems principle the ground state. DFT in principal gives a good description of ground state properties. Practical application s of DFT is based on approximations for so called exchange co-relation potential. The exchange describes the effects of the Pauli principle and the coulomb potential

beyond pure electrostatic interactions of the electrons. A common local density approximation (LDA) which locally substitutes the exchange co-relation energy density of an inhomogeneous system by that of an electron gas evaluated at the local density. (85) LDA calculations predict that pure Fe pnictide of both 1111 and 122 classes possess a ferromagnetic instability due to very high density of states. In the Fe-As layers, the Fe atoms are bonded with four As atoms in tetrahedron for both families. The Fermi surface and band structure of these compound are similar. The band around the Fermi level for both compounds is mainly formed by Fe-d orbitals. We can see from Figure (3.5), the Fe 3d orbitals are the main contributors to the density of states together with the very small contribution from As-p orbital. The states at the Fermi levels have contributions from spin d_{yz} and $d_{x^2y^2}$ orbitals. In this sense we can say that all phenomena related to superconductivity in these compounds take place in the square lattice of Fe within the FeAs layer and $dx^2 - y^2$ orbitals. In this sense we can say that all phenomena related to superconductivity in these compounds take place in the square lattice of Fe within the FeAs layer.

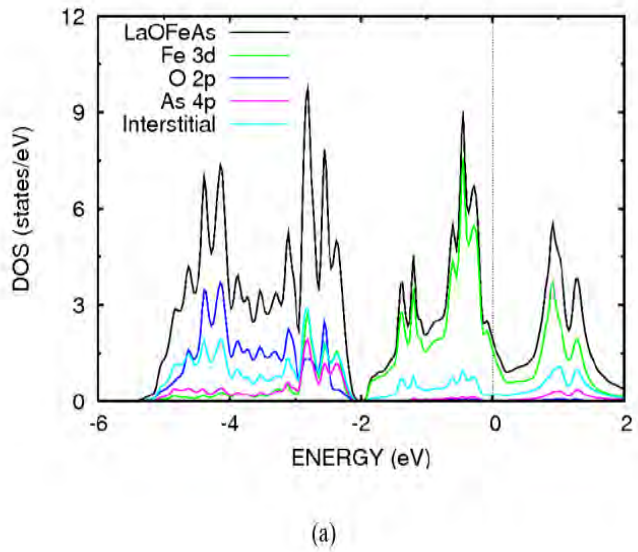

Figure 3.5:

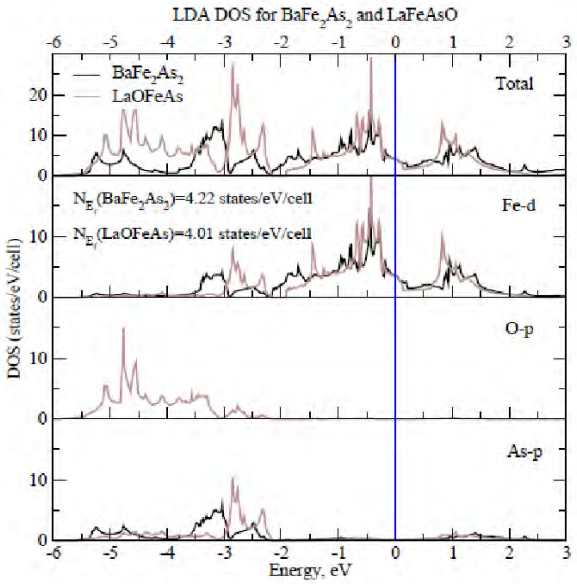

(b)

Figure 3.6: (a) LDA DOS (44) for LaOFeAs The total and partial LDA DOS for BaFe2As2 (black lines) and LaOFeAs compound (85)

The available electronic structure calculations of Fe oxypnictide convey the key information that all five Fe 3d are located at the Fermi level this is different than cuprates. There are five sections of the Fermi surface two concentric hole pockets Γ_2 and Γ_1 centered at $\Gamma[k = (0, 0)]$ point which are hole type Fermi surface and mostly come from dyz and dzx states of Fe. In addition the electron elliptical pocket centered at $M[k = (\pi, \pi)]$, mostly come from the dxy and $\frac{dyz}{zx}$ states of Fe. The shape of ellipse comes from the hybridization between dxy and dyz . The stronger the hybridization, the more the distortion of the ellipse. These ellipses have the same size but turned are in to 90^0 to each other. There is one 3d hole band with spherical Fermi Surface around z point the last one vanishes upon doping, which is the smallest one and usually neglected in the analysis of superconducting pairing because of its smaller space volume it is believed that its contribution to the electronic properties is comparatively smaller (85)

It is clear that this kind of a band structure shown in the Figure (3.6) leads to similar

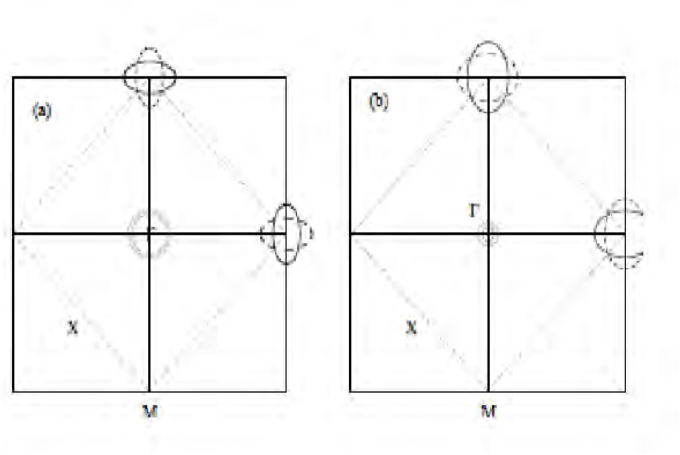

Figure 3.7: schematic plots for Fermi surfaces of LaOFeAs, Figure (a) is for pure LaOFeAs and Figure (b) is for LaOFeAs with 20 % F-doping. The large square represented the brillouin zone for one Fe cell, while the small diamond is the brillouin zone for two Fe cell. Figure (b) shows the electron for doped distorted ellipses as compare to the Figure (a).(86)

Fermi surfaces of 1111 and 122 compounds, as it is shown in the Figure (3.7). As mentioned earlier there are three hole like cylinders at the center of Brillouin zone and two electron like at the corners. The almost cylindrical form of the Fermi surface reflects the quasi two dimensional nature of the electronic spectrum in these new superconductors. The brillouin zones for the two types of compounds are similar with a slight difference due to their lattice parameters.Apart from the common general features in their electronic structures, many differences may exit between the different families and even in the same family as we shall see below. In this section, one can point out similarities and differences of the compound LaFeASO and LaFePO, Both LaFePO and LaFeAsO have similar crystal structures however, they show different transport, magnetic and superconducting properties with great difference in the transition temperature T_c , being very low ($\sim 5 - 8K$) in the former and may reach up to $\sim 26K$ in the latter. In this section, we can see the results of first-principles calculations performed by V. Vildosola et al. [93] in which a comparative study between the these two compounds was performed in order to clarify the relations between electronic properties and the electronic structure of these

materials. Fig. 3.8 shows the obtained band structures for both materials using experimental crystal structure. It is clear that the bands near the Fermi level which correspond to Fe, have larger bandwidth in LaFePO as compared to LaFeAsO. This is a plausible explanation of why the former is observed to be a better metal (in the sense of smaller resistivity). This also indicates a less degree of electronic correlations in LaFePO.

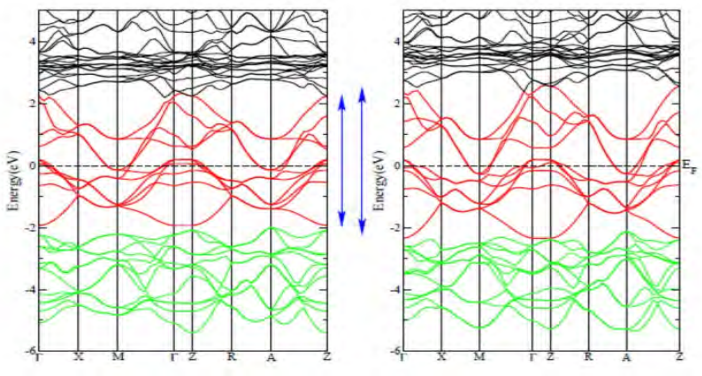

Figure 3.8: Band structure of LaFeAsO (left) and LaFePO (right). Red and green bands have mainly Fe 3d and Pnictogen/Oxygen p character respectively [93]

Fig. 3.9 shows the very low-energy band structure and Fermi surfaces of both compounds (calculated for the experimental crystal structure). In both compounds, the Fermi level is crossed by five bands with mainly Fe character. Both materials present two electron pockets centered at M and two hole pockets centered at Γ with mainly d_{xz} and $d_{\frac{xz}{yz}}$ character. The significant difference between these compounds comes from the third pocket centered along the $\Gamma \rightarrow Z$ line direction. In LaFeAsO, this third pocket has mainly d_{xy} character and presents almost no dispersion along the z-direction (it is therefore two dimensional in nature). In contrast, in LaFePO, it consists of a dispersing 3D pocket with mainly $d_{3z^2r^2}$ character. These difference appear clearly in the Fermi surfaces plots (right-hand side of Fig. 3.9. The explanation of this difference in the low energy band structure, as obtained from first-principles electronic structure methods, lies mainly in its great sensitivity to the Fe-Pn distance and to the vertical distance of the Pn to the Fe plane. The reason for this sensitivity is that, close to the Fermi level, there is a sizeable

hybridization between Fe and Pn states.

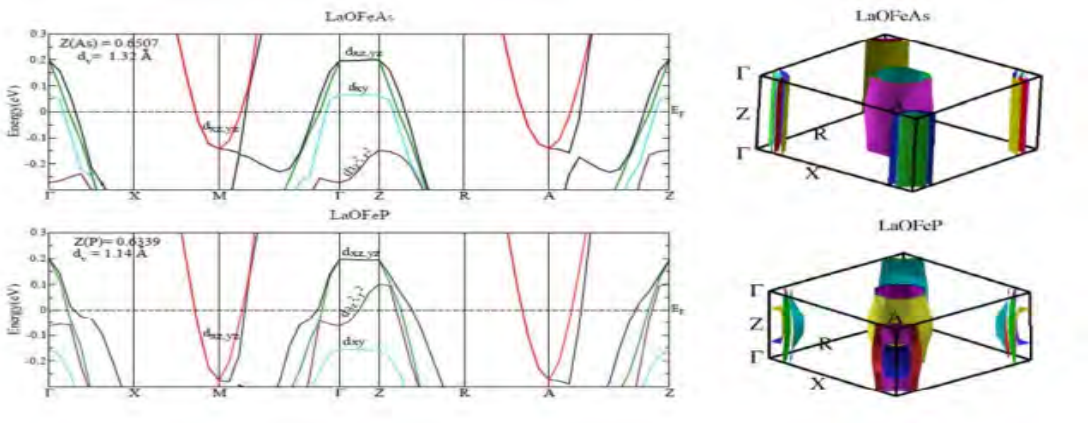

Figure 3.9: Low energy region of LaFePns band structures and their corre- sponding Fermi surfaces plots calculated at their experimental crystal structure with Pn=As (upper panel) and P (lower panel) [38]. [93]

In order to understand better the sensitive dependence of the low-energy bandstructure on the Pn height with respect to the Fe plane, the expermentst studied the LaFeAsO system by fixing the lattice parameters a and c at their experimental values, while varying the vertical position of As all the way down to a position which is very close to the one that P has in LaFePO material. We notice that the 2D pocket with d_{xy} character in the experimental LaFeAsO (upper panel) evolves into a 3D pocket with $d3z^2 - r^2$ character as As is moved closer to the plane (lower panel). Therefore, one can say that LaFeAsO evolves into LaFePO as the height of As to the Fe plane decreases.

The density of states (DOS) for holes and electrons is comparable for undoped material, but with doping either holes or electrons become dominant. The undoped compounds show the structural (tetragonal to orthorhombic) phase transition and magnetic transition is attributed to spin density wave (SDW) formation due to the nesting of the Fermi surfaces. Doping suppresses this long range magnetic order, which is believed to be prerequisite for superconductivity in Fe based superconductors. Supercondtivity arises due to destruction of magnetic coupling between the layers.

In the superconducting state, the electrons pair and condense into a low energy state

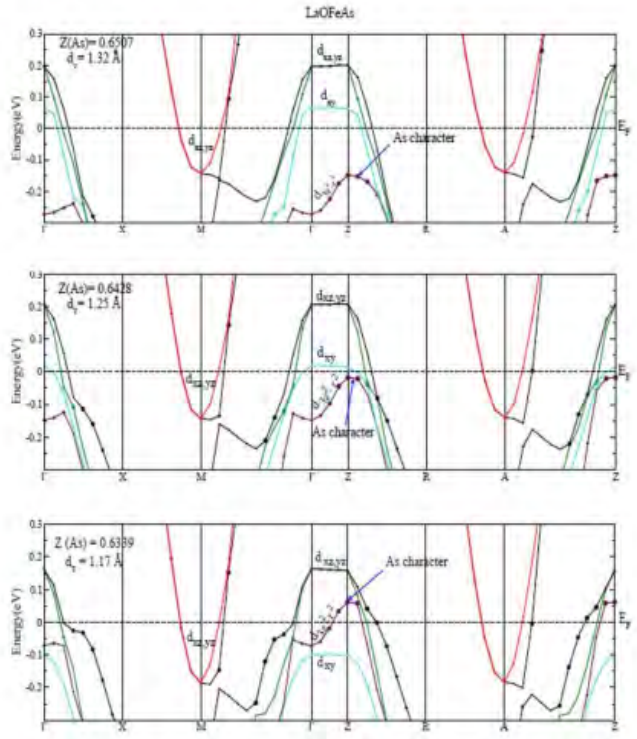

Figure 3.10: Sensitivity of the low energy band structure for LaFeAsO to d_v (As's vertical distance with respect to the Fe plane) for fixed lattice constants a and c. The considered d_v values are indicated in each plot [93].

leading to the formation of a gap at the Fermi energy E_f. It is this gap that protects the superconducting condensate. A perfectly symmetrical gap which is equally spaced above and below the Fermi level is a strong indication that electrons are paired up. That superconducting gap exists at and below the transition temperature. One of the most prominent differences when comparing high-temperature superconductivity with metallic superconductors is that the symmetry of the superconducting order parameter is d-wave like in cuprates. In BCS theory the order parameter coincides with half of the total energy gap $2\Delta k$ in the electronic density of states. Hence the quasi particle dispersion exhibits gapless nodes at the Fermi surface along the diagonals of the Brillouin zone. Based on the general space group of the material, and together with the detailed pairing interaction between the two electrons, the superconducting gap should have a specific symmetry for an individual superconductor

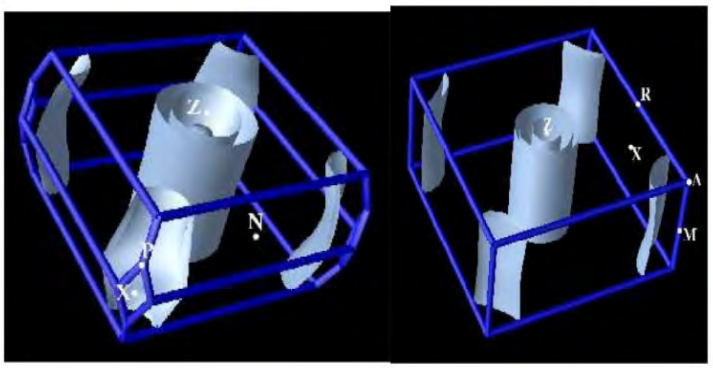

Figure 3.11: The Fermi surfaces for BaFe2As2 (left side) and for LaOFeAs (right side) (85)

Angle Resolved Photo Emission Spectroscopy is one of the most direct methods of studying the electronic structure of the surface of solid .The angle resolved photoemission spectroscopy (ARPES) technique is the reliable technique to measure not only the Fermi surface but also the superconducting gap. There are already a number of papers, where the electronic spectrum and Fermi surfaces in these new superconductors were studied using the angle resolved photoemission spectroscopy (ARPES) technique. But comparatively less amount of work has been done on 1111 type due to lack of nice single crystals in this type of superconductors. The different gaps have been observed in several compound classes by a variety of experiments. (ARPES) measurement has been done on the $NdO_{0.9}F_{0.1}FeAs$ system. The momentum dependence of the superconducting gap in the hole pocket around $\Gamma(0,0,0)$and cylindrical electron pocket at each corner of the Brillouin zone (M) was estimated from this and found to measurement have a magnitude of 20 meV.

Anothers measured ARPES on single crystals of the $Ba_{0.6}K_{0.4}Fe_2As_2$ superconductor with $T_c = 35K$ and found the multiple nodeless superconducting gap (22). They observed multiple Fermi surface sheets in this compound. Two hole-like Fermi surface sheets around the Γ point exhibit different superconducting gaps. An inner Fermi surface showed large gap of$\Delta = 12meV$, which is slightly momentum dependent while the outer

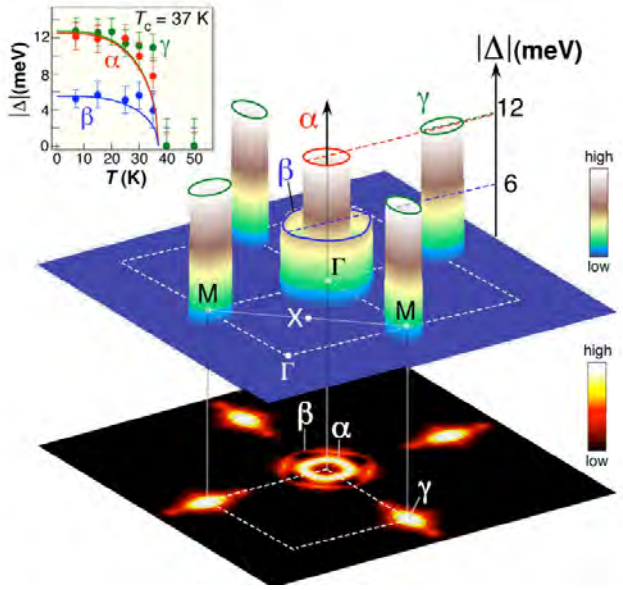

Figure 3.12: ARPES intensity map as a function of kx and ky momentum, integrated within 20 meV of the Fermi energy. Bright areas mark the location of the Fermi surface.(87)

Fermi surface shows the smaller gap ofΔ = 7to 8 meV, which is nearly isotropic. Similar results were found in the ARPES measurement on $Ba_{0.6}K_{0.4}Fe_2As_2$, $T_c = 37$ shows two superconducting gaps. A large one at $\Delta = 12meV$ on small hole like cylinder around Γ and also hole like cylinders around point M and small one $\Delta = 6meV$ on big hole like cylinder around Γ point . Both gaps are nearly isotropic on specific Fermi surface sheets. These results of nodeless gaps are corresponding to the generalized S wave pairing (89). The above Figure (3,12) shows the three dimensional picture of the superconducting gap of size Δ in $Ba_{0.6}K_{0.4}Fe_2As_2$. The inset shows the temperature dependence of the gap on different Fermi surfaces. The above ARPES measurements have been performed for both 1111 and 122 materials. They demonstrated the existence of a well defined Fermi surface that consists of hole and electron pockets which is in agreement with the predictions of electronic structure calculation. [45] A number of different scenarios have been proposed to explain the mechanism of the superconductivity in Fe based systems, with predictions about the symmetry of the order parameter ranging from isotropic and anisotropic s-wave

to d-wave and p-wave symmetry. Conventional electron-electron interaction mediated by phonon intraction,in the electron mechanisim superconductivity arises from electron- electron repulsion where spin and charge fluctuation mediated pairing. Since that repulsion act as an atraction when Δ_k changes sign across the typical momentum transfer.
The spin fluctuation(SF) spectrum usually reach for this compound and come from three separete sources

- The system relatively close to stoner ferromagnetic instablity.fig.(3.13)
- There is a nearest-neighbor antiferromagnetic (AFM) super exchange fig.(3.13)
- There are nesting related AFM spin density wave type SFs near wave vector connecting the electron and hole pocket.This appear to be stronger one

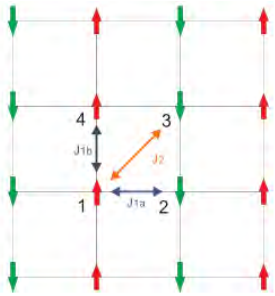

Figure 3.13: (Color online) Spin arrangment and exchange inter actions in the Fe plane of the striped AFM phase. The arrows on lattice sites indicate the Fe spin directions. The double arrows indicate the nearest neighbor AFM interaction (J_{1a}), FM interaction (J_{1b}) and next nearest neighbor AFM interaction (J_2) (94).

Fig. 3.13 shows the spin structure of the Fe plane which is common to the all these materials. From here on we use the $(\pi, 0)$ striped AFM coordinate system, which is convenient to discuss the spin wave dispersions. Magnetic interactions between Fe moments are governed by two dominating AFM couplings J_{1a} and J_2 , and the FM nearest-neighbor exchange J_{1b} is small.

The band structure first appear intractably complex with five orbital symetries $1.d_{3z^2-R^2}$, $2.d_{xz}$,$3.d_{yz}$,$4.d_{x^2-Y^2}$, $5.d_{xy}$ but it is in fact relatively simple evolving three Fe orbitals near

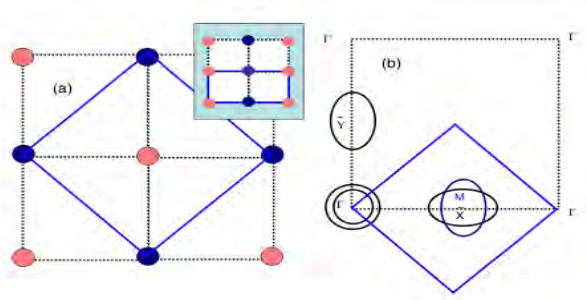

Figure 3.14: (color online). Fermi surface formation upon backfold- ing of the large BZ corresponding to a simple Fe square lattice. (a) Real space: the four small unit cells of the Fe-only sublattice (dashed lines) with the larger solid diamond of actual two-Fe unit cell. Dark and light circles indicate superexchange (checker board) ordering . The inset shows the spin-density wave corre sponding to X point SFs. (b) Reciprocal space: the dashed black square is the unfolded BZ, the solid blue diamond is the down- folded zone, and the blue ellipse is the electron pocket from the Y point downfolded onto the X point (which is M in the small BZ)(95)

fermi level.The hole pocket around Γ originate from Fe d_{xz} and d_{yz} bands that are degenerate at Γ and form two nearly perfect concenteric cylinder and two electron pockets around X and Y formed by d_{yz} and d_{xz} .This bands hyberdize with band $d_{x^2-Y^2}$. up on hyberdization these two bands yield an oval cylinderical electron pocket elongated along ΓX and ΓY

The Fermi surface consists of four pieces two concentric hole pockets (denoted as α_1, α_2) $(k_x, k_y) = (0, 0)$, two electron pockets around $(\pi, 0)(\beta_1) or (0, \pi)(\beta_2)$, respectively. $\alpha i \beta i$ corresponds to the Fermi surface around the Γ Z(MA) line (in the original BZ) . The orbital character is again entangled: α and portions of β near BZ edge have mainly d_{XZ} and d_{YZ} character, while the portions of β away from the BZ edge and γ have mainly $d_{x^2-y^2}$ orbital character.

The spin susceptibility has peaks around $(k_x, k_y) = (\pi, 0), (0, \pi)$ (i.e., a colinear SDW), which reflects the Fermi surface nesting around $\sim (\pi, 0), (0, \pi)$ across α and and also β and in Fig.3.15. The spin structure is consistent with the neutron scattering experiments in which the colinear structure is observed at low temperatures for the undoped case.[90] For superconductivity, we show in Fig .3.16 the diagonal elements of the gap function

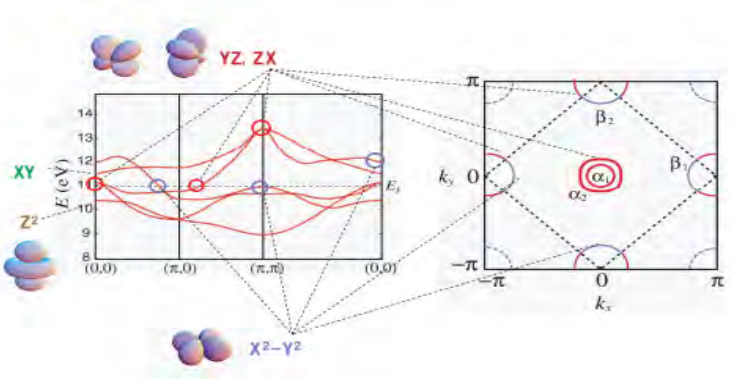

Figure 3.15: (color online) The band structure of the five band model in the unfolded BZ, where the inter layer hoppings are included. Orbital character is indicated for the bands and for the Fermi surface (right panel, with the original (dashed lines) and the unfolded (solid) BZ indicated). Bottom panels depict (two equivalent realisations of) the colinear SDW.(95)

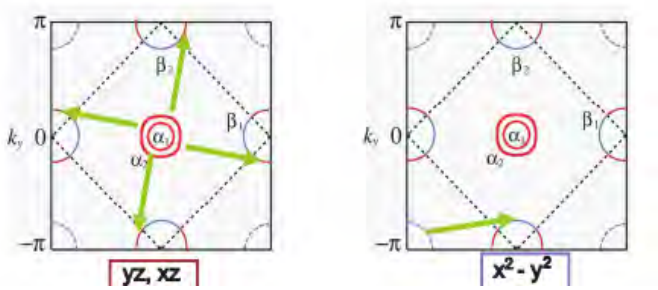

Figure 3.16: (color online) Bottom panels: Diagonal elements of the gap function matrix in the orbital representation for the XZ, Y Z (left) and $X^2 - Y^2$ (right) in the 5-band RPA for 10% doped $LaFeAsO_{1x}F_x$ for the same parameter set as in the previous figure. Nesting vectors are indicated.(95)

matrix for or- bitals d_{YZ} , d_{ZX} , and $d_{X^2-Y^2}$. The gap is a curious extended s-wave,[40,3] where the gap changes sign across the $\alpha - \beta or \beta - \gamma$ nesting vector $\sim (\pi, 0), (0, \pi)$at which the spin fluctuations develop.for the multiband system, the magnitude of gap of the $d_{x^2-y^2}$ orbital turns out to be large compared to other orbitals, which indicates that the $d_{y^2-y^2}$ orbitals play the main role in the superconductivity.

As opposed to undoped material we do not find any FM solution for doped compound,this sudjests that the main function of dopping is to move the system away ferromagnetic instablities, that the system become less magnetic is due to the fact that up on doping

the heavy 3D hole pocket nearΓ rapidly filled and the total density of state (DOS) drops. these the fermiology found in doped LaFeAsO gives rise to antiferromaginetic spin fluctuation while tendency to magnetisim existing at zero doping is supressed.

3.7 Antiferromagnetic order

Since superconductivity in iron pnictides appear by doping their parent compounds with charge carriers, it is natural to wonder what the ground states of the parent compounds are. Also an anomaly in the resistivity of the parent compounds of these materials occur below a certain temperature ($\sim 150K$ in the case of LaFeAsO) in addition to a small anomaly in the magnetic susceptibility. Optical conductivity and theoretical calculations suggest that LaFeAsO exhibits a spin-density-wave (SDW) instability that is suppressed by doping with electrons to induce superconductivity.However, the first direct evidence of SDW order in LaFeAsO came from neutron-scattering experiments by de. la Cruz et al. [91]. These experiments demonstrated that LaFeAsO undergoes an abrupt structural distortion below $\sim 155K$, changing the symmetry from tetragonal (space group$\frac{P_4}{nmm}$) to monoclinic (space group$\frac{P112}{n}$) at low temperatures, and then, at $\sim 137K$, develops long-range SDW-type antiferromagnetic (AFM) order with a small moment but simple magnetic structure. The magnetic structure is consistent with theoretical predictions, but the moment of $0.36\mu B$ per iron atom observed here at 8 K is much smaller than the predicted value of$\sim 2.3\mu B$ per iron atom. Later, the AFM order in $BaFe_2As_2$ was also observed by a neutron diffraction study by Huang et al. [92]. Similar to the case of LaFeAsO, $BaFe_2As_2$ shows a tetragonal-to-orthorhombic distortion structural transition and magnetic transition. However, both transitions occur simultaneously in $BaFe_2As_2$ in contrast with the separated transitions observed previously in LaFeAsO. These results for both compounds are summarized in Fig. 3.17.

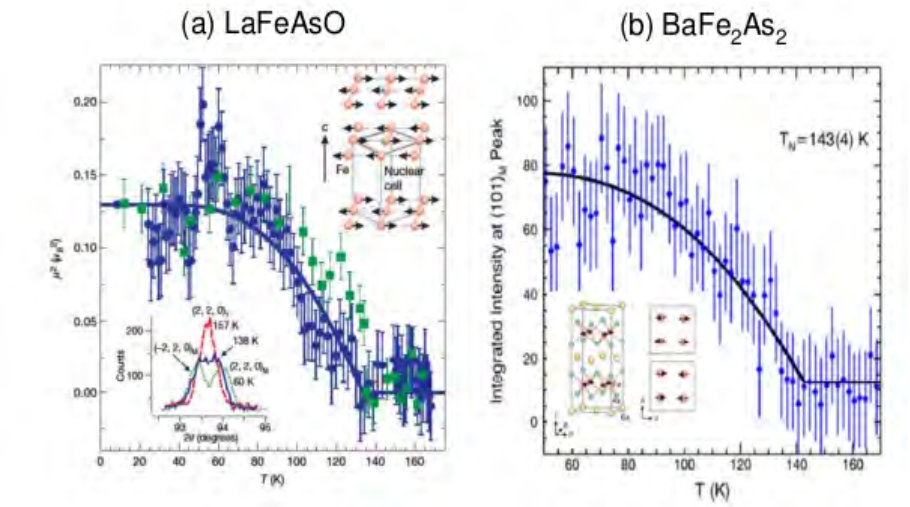

Figure 3.17: Antiferromagnetic ordering in (a) LaFeAsO [91] and (b) $BaFe_2As_2$ [92].

3.8 Similarities and differences with cuprates

The excitement with this discovery was largely stimulated with some close similarities and diferences between iron-based SC and HTSC:

⇒ Smilarties

- Both systems are layered in structure ($Cuo_2\ V_s\ FeAs$).
- Parent compounds are antiferromagnets and superconductivity appears upon doping which exceeds critical value. At the same time antiferromagnetic phase is suppressed.
- The phase diagrams are similar.
- Both are type II superconductors.
- Both have d- electron in key role (Cu Vs Fe)

thus , the iron pnictides are multi-band systems in contrast to cuprates which are single-band systems however the parent compound of cuprates is a Mott insulator and that of iron pnictides is a bad metal or semiconductor.

Chapter 4

Conclusion

Iron pnictides are high critical temperature not exeeding 55K and they took the attention of reaserchers becaouse of their structural similarities with copper oxides since both have antiferomagnetic phase next to superconductivity.Pnictides are not phonon-mediated superconductors hence, they are unconventional and electron-phonon coupling constant $\lambda = 0.21$ which is too small to express such critical temperature.The microscopic pairing mechanisim for iron pnictide seems spin fluctuation becuose the nesting of fermi surfaces around $(\pi, 0), (0, \pi)$ and structural distortion and magnetic order vanish in F doping and SDW suppresed before superconductivity for most cases.On the other hand superconductivity can coexist with SDW.This shows that pairing mechanisim for iron pnictide high tempratur superconductivity is not general case like BCS theory in conventional superconductivity which is phonon mediated.Pnictides of differnt famlies have common general; featers like layers of (FeAs) in stracture and similar fermi surfaces of electronic structur.Beside this differences may exisit with silmilar famlies ,the vertical distance of of Pn to Fe plane is diffent in comparsion with the two compounds LaFeAsO and LaFePOwith T_c 26K in the former and $\sim (5K - 7K)$ in the latter LaFeAsO evolves to LaFePO as the height of As to Fe plane decreases .This indicates that another mechanisim can be found in future in addition to known mechanisims of raising T_c. .

Bibliography

[1] W. Meissner and R. Ochsenfeld, Naturwiss. **21**, 787 (1933).

[2] F. London and H. London, Proc. Roy. Soc. (London) **149**, 71 (1935).

[3] H. Kamerlingh Onnes, Leiden Comm. **120b**, **122b**, 124c (1911).

[4] V. L. Ginzburg and L. D. Landau, Zh. Eksp. Teor. Fiz. 20, 1064, (1950).

[5] A. A. Abrikosov, Zh. Eksp. Teor. Fiz. **32**, 1442 (1957).

[6] E. Maxwell, Phys. Rev. **78**, 477, (1950).

[7] C. A. Reynolds, B. Serin, W. H. Wright, (1950).

[8] J. Bardeen, L. N. Cooper, and J. R. Schrieffer, Phys. Rev. **108**, 1175, (1957).

[9] N. N. Bogoliubov, Zh. Eksp. Teor. Fiz. **34**, 58, (1958)..

[10] L. P. Gorkov, Zh. Eksp. Teor. Fiz. **36**, 1918, (1959)..

[11] J. G. Bednorz and K. A. M ller, Z. Physik **B 64**, 189 ,(1986).

[12] M. Wu, J. Ashburn, C. Torng, G. Peng, F. Szofran, P. Hor, and C. Chu, Phys.Rev. Lett. **58**, 908, (1987).

[13] V. Z. Kresin, S. A. Wolf, Rev. Mod. Phys. **81**, 481, (2009)

[14] Y. Kamihara, T. Watanabe, M. Hirano, and H. Hosono, J. Amer. Chem. Soc. **130**, 3296, (2008).

[15] G. F. Chen, Z. Li, D. Wu, G. Li, W. Z. Hu, J. Dong, P. Zheng, J. L. Luo, andN. L. Wang, Phys. Rev. Lett. **100**, 247002, (2008).

[16] Z.-A. Ren, J. Yang, W. Lu, W. Yi, G.-C. Che, X.-L. Dong, L.-L. Sun, and Z.-X.Zhao, *Materials Research Innovations* **12**, 105, (1994)

[17] Z.-A. Ren, J. Yang, W. Lu, W. Yi, X.-L. Shen, Z.-C. Li, G.-C. Che, X.-L. Dong,L.-L. Sun, F. Zhao, and Z.-X. Zhao, Europhys. Lett. **82**, 57002, (2008)..

[18] V. V. Moshchalkov, V. Bruyndoncx, E. Rosseel, L. Van Look, M. Baert, M. J. Van

Bael,T. Puig , C. Strunk and Y. Bruynseraede , Rev. Lett. **100**, 247002, (2008)"

[19] X. H. Chen, T. Wu, G. Wu, R. H. Liu, H. Chen, and D. F. Fang, Nature **453**,761 ,(2008).

[20] P. Cheng, L. Fang, H. Yang, X. Zhu, G. Mu, H. Luo, Z. Wang, and H.-H. Wen,Science in China G **51(6)**, 719-722 ,(2008).

[21] F. J. Morin and J. P. Maita, *"Electrical properties of silicon containing arsenic and boron"*, Physical Review, vol. 96, pp. 2835, (1954).

[22] G. E. Stillman, C. M. Wolfe, and J. O. Dimmock, *"Hall coefficient factor for polar mode scattering in n-type GaAs", Journal of Physics and Chemistry of Solids,* vol. **31**, pp. 11991204, (1970).

[23] S. J. Crowe, S. B. Dugdale, Zs. Major, M. A. Alam, J. A. Duffy and S. B.Palmer, Europhys. Lett. **65**, 235, (2004)

[24] G. F. Chen, Z. Li, D. Wu, G. Li, W. Z. Hu, J. Dong, P. Zheng, J. L. Luo, and N. L. Wang, Phys. Rev. Lett. **100**, 247002, (2008).

[25] Z.-A. Ren, J. Yang, W. Lu, W. Yi, G.-C. Che, X.-L. Dong, L.-L. Sun, and Z.-X.Zhao, *Materials Research Innovations* **12**, 105, (2008).

[26] X. H. Chen, T. Wu, G. Wu, R. H. Liu, H. Chen, and D. F. Fang, Nature 453,761, (2008).

[28] Z.-A. Ren, G.-C. Che, X.-L. Dong, J. Yang, W. Lu, W. Yi, X.-L. Shen, Z.-C.Li, L.-L. Sun, F. Zhou, and Z.-X. Zhao, Europhys. Lett. **83**, 17002 ,(2008)..

[29] P. Cheng, L. Fang, H. Yang, X. Zhu, G. Mu, H. Luo, Z. Wang, and H.-H. Wen,Science in China G **51(6)**, 719-722, (2008)..

[30] C. Wang, L.-J. Li, S. Chi, Z.-W. Zhu, Z. Ren, Y.-K. Li, Y.-T. Wang, X. Lin,Y.-K. Luo, S. Jiang, X.-F. Xu, G.-H. Cao, and Z.-A. Xu, Europhys. Lett **83**,67006, (2008).

[31] Z.-A. Ren, W. Lu, J. Yang, W. Yi, X.-L. Shen, Z.-C. Li, G.-C. Che, X.-L. Dong,L.-L. Sun, F. Zhou, and Z.-X. Zhao, Chin. Phys. Lett. **25**, 2215 ,(2008).

[32] 'M. Rotter, M. Tegel, and D. Johrendt, Phys. Rev. Lett. **101**, 107006, (2008).

[33] K. Sasmal, B. Lv, B. Lorenz, A. M. Guloy, F. Chen, Y. Y. Xue, and C. W.Chu, Phys. Rev. Lett. **101**, 107007 ,(2008)

[34] M. S. Torikachvili, S. L. Budko, N. Ni, and P. C. Canfield, Phys. Rev. Lett. **101**, 057006 ,(2008).

[35] J. H. Tapp, Z. J. Tang, B. Lv, K. Sasmal, B. Lorenz, P. C.W. Chu, and A. M.Guloy, Phys. Rev. B **78**, 060505(R), (2008).

[36] D. R. Parker, M. J. Pitcher, P. J. Baker, I. Franke, T. Lancaster, S. J. Blundell,and S. J. Clarke, Chem. Commun. (Cambridge) ,, **2189**.(2009),

[37] S. Matsuishi, Y. Inoue, T. Nomura, M. Hirano, and H. Hosono, J. Phys. Soc.Jpn. 77, 113709, (2008).

[38] C. de la Cruz, Q. Huang, J. W. Lynn, J. Li, W. Ratcliff, J. L. Zaretsky, H. A.Mook, C. F. Chen, J. L. Luo, N. L. Wang, and P. Dai, Nature **453**, 899, (2008).

[39] M. A. McGuire, A. D. Christenson, A. S. sefat, R. Jin, E. A. Payzant, B. C.Sales, M. D. Lumsden, and D. Mandrus, Phys. Rev. B **78**, 094517, (2008).

[40] K. Kitagawa, N. Katayama, K. Ohgushi, M. Yoshida, and M. Takigawa, J.Phys. Soc. Jpn. **77**, 114709 ,(2008).

[41] S.-H. Baek, N. J. Curro, T. Klimczuk, E. D. Bauer, F. Ronning, and J. D.Thompson, Phys. Rev. B **79**, 052504 ,(2009).

[42] Z. P. Yin, S. Leb'gue, M. J. Han, B. P. Neal, S. Y. Savrasov, and W. E. Pickett Phys. Rev. Lett. **101**, 047001, (2008)..

[43] T. Yildirim, Phys. Rev. Lett. **101**, 057010, (2008)..

[44] R. H. Liu, T. Wu, G. Wu, H. Chen, X. F. Wang, Y. L. Xie, J. J. Yin, Y. J.Yan, Q. J. Li, B. C. Shi, W. S. Chu, Z. Y. Wu, and X. H. Chen, Nature **459**, 64,(2009)..

[45] Neil W.Ashcroft, N.D.Mermin, Solid State Physics, Holt,Rinehartand Winston, 1975..

[46] A. A. Abrikosov, *On the magnetic properties of superconductors of the second group*,Zh. Eksp. Teor. Fiz., **32**, 1442 (1957); Sov. Phys. JETP, 5, 1174 ,(1957)

[47] L. Pitaevskii, *Superconductivity: Volume 1, Conventional and unconventional superconductors*, editted by K. H. Bennemann and J. B. Ketterson (Springer) ,(2008)

[48] V. V. Schmidt, *The physics of superconductors (Springer)* ,(1997)

[49] Emanuel Maxwell, *Isotope Effect in the Superconductivity of Mercury*, Phys. Rev., **78**,477, (1950)

[50] C. A. Reynolds, B. Serin, W. H. Wright, and L. B. Nesbitt, *Superconductivity of Isotopes of Mercury*, Phys. Rev., **78**, 487 ,(1950).

[51] G. M. Eliashberg, *Interactions between electrons and lattice vibrations in a superconductor*, Zh. Eksp. Teor. Fiz., **38**, 966 (1960); Sov. Phys. JETP, 11, 696, (1960)

[52] H. Frohlich, *Interaction of Electrons with Lattice Vibrations*, Proc. R. Soc. Lond. A, **215**,291 ,(1952).

[53] L. N. Cooper, Bound Electron Pairs in a Degenerate Fermi Gas, Phys. Rev., **10**4, 1189,(1956).

[55] K. H. Bennemann and J. B. Ketterson, *Superconductivity: Volume 1, Conventional and unconventional superconductors*, editted by K. H. Bennemann and J. B. Ketterson (Springer), (2008)

[56] C. Wang, L. Li, S. Chi, Z. Zhu, Z. Ren, Y. Li, Y. Wang, X. Lin, Y. Luo,S. Jiang, Z. Xu, G. Cao, and Z. Xu: Euro Phys. Lett. **83** ,(2008), 67006.

[57] X. H. Chen, T. Wu, G. Wu, R. H. Liu, H. Chen, and D. F. Fang: Nature **453** 761,(2008) .

[58] G. F. Chen, Z. Li, D. Wu, G. Li, W. Z. Hu, J. Dong, P. Zheng, J. L. Luo,and N. L. Wang: Phys. Rev. **Lett** 100 ,247002,(2008) .

[59] Z.-A. Ren, J. Yang, W. Lu, W. Yi, X.-L. Shen, Z.-C. Li, C.-C. Che, X.-L.Dong, L.-L. Sun, F. Zhou, and Z.-X. Zhao: Euro Phys. Lett. **82** ,57002,.(2008)

[60] Z.-A. Ren, J. Yang, W. Lu, W. Yi, G.-C. Che, X.-L. Dong, L.-L. Sun,Z.-X. Zhao: Materials Research Innovations **12** , 105.(2008)

[61] M. Rotter, M. Tegel, I. Shellenberg, W. Hermes, R. Pottgen, and D.Johrendt: Phys. Rev. **B 78** 020503.(2008)

[62] M. Rotter, M. Tegel, and D. Johrendt: Phys. Rev. Lett. **101** (2008)107006.

[63] G. F. Chen, Z. Li, G. Li, W. Z. Hu, J. Dong, X. D. Zhang, P. Zheng, N.L. Wang, and J. L. Luo: Chin. Phys. Lett **25** , 3403.(2008)

[64] K. Sasmal, B. Lv, B. Lorenz, A. Guloy, F. Chen, Y. Xue, C. W. Chu:Phys. Rev. Lett 101 107007. (2008)

[65] G. Wu, H. Chen, T. Wu, Y. L. Xie, Y. J. Yan, R. H. Liu, X. F. Wang, J.J. Ying, and X. H. Chen: J. Phys.: Condens. Matter **20** 422201.(2008)

[66] H. S. Jeevan, Z. Hossain, C. Geibel, P. Gegenwart: Phys. Rev. B **78** 092406.(2008)

[67] A. S. Sefat, R. Jin, M. A. McGuire, B. C. Sales, D. J. Singh, and D.Mandrus: Phys. Rev. Lett **101** 117004.(2008)

[68] X.C. Wang, Q.Q. Liu, Y.X. Lv, W.B. Gao, L.X. Yang, R.C. Yu, F.Y. Li,C.Q. Jin: Solid State Communications **148** 538.(2008)

[69] F.-C. Hsu, J.-Y. Luo, K.-W. Yeh, T.-K. Chen, T.-W. Huang, P. M. Wu,Y.-C. Lee, Y.-L. Huang, Y.-Y. Chu, D.-C. Yan, and M.-K. Wu: Proc.Natl. Acad. Sci. USA **14262**.(2008)

[70] H. Takahashi, K. Igawa, K. Arii, Y. Kamihara, M. Hirano, and H. Hosono:Nature **453** , 376.(2008)

[71] M. Rotter, M. Tegel, and D. Johrendt: Phys. Rev. Lett. 101 107006.(2008)

[72] K. Miyazawa, K. Kihou, P. M. Shirage, C.-H. Lee, H. Kito, H. Eisaki, and A. Iyo: J. Phys. Soc. Jpn. **78** 034712.(2009)

[73] C. de la Cruz et.al., Nature **453**, 899 (2008) (10.2.2009)

[74]Kamihara et. al., JACS **128**, 10012 (2006) (2.3.2009)

[75]Sasmal K, Lv B, Lorenz B, Guloy A M, Chen F, Xue Y Y andChu C W 2008 *Superconducting Fe-based compounds*$(A_{1x}Sr_x)Fe_2As_2$ *with A = K and Cs with transitiontemperatures up to 37 K* Phys. Rev. Lett. **101** 107007

[76]De la Cruz C et al *Magnetic order close to superconductivity in the iron-based layered* $LaO_{1x}F_xFeAs$ *systems* Nature **453** 899902 (2008)

[77]McGuire M A et al *Phase transitions in LaFeAsO: structural, magnetic, elastic, and transport properties, heatcapacity and M ssbauer spectra Phys. Rev. B* ***78*** *094517(2008)*

[78] *Rotundu C R, Keane D T, Freelon B, Wilson S D, Kim A,Valdivia P N, Bourret-Courchesne E and Birgeneau R J Phase diagram of the* $PrFeAsO_{1x}F_x$ *superconductorarXiv:0907.1308 (2009)*

[79]*Drew A J et al Coexistence of static magnetism and superconductivity in* $SmFeAsO_{1x}F_x$ *as revealed by muonspin rotation Nat. Mater. 8 3104 (2009)*

[80]*Margadonna S, Takabayashi Y, Mcdonald M T, Brunelli M,Wu G, Liu R H, Chen X H and Prassides K Crystalstructure and phase transitions across themetalsuperconductor boundary in the* $SmFeAsO_{1x}F_x(0 < x < 0.20)$*family* Phys. Rev. B **79** 014503 (2009)

[81] C. W. Chu and B. Lorenz. *High Pressure Studies on Fe-Pnictide Superconductors.*arXiv0902.0809iv:

[82] Hideto Fukazawa, Kenji Hirayama, Kenji Kondo, Takehiro Yamazaki, Yoh Kohori,Nao Takeshita, Kiichi Miyazawa, Hijiri Kito, Hiroshi Eisaki, Akira Iyo. 75*As NMR study ofthe ternary iron arsenide* $BaFe_2As_2$:arXiv: 0806.4514

[83] D. J. Singh, M. H. Du, *$LaFeAsO_{1x}F_x$: A low carrier density superconductor near-itinerant magnetismarXiv*:0803.0429

[84] I. A. Nekrasov, Z. V. Pchelkina, M. V. Sadovskii .*Electronic Structure of PrototypeAFe_2As_2 and ReOFeAs High-Temperature Superconductors*: aComparisonarxiv:0806.2630v2 ,(2008)

[85] I. A. Nekrasov, Z. V. Pchelkina, M. V. Sadovskii. *Electronic Structure of PrototypeAFe_2As_2 and ReOFeAs High-Temperature Superconductors*: a Comparison:

[86] Hai-Jun Zhang, Gang Xu, Xi Dai and Zhong Fang. *Enhanced Orbital Degeneracy inMomentum Space for LaOFeAs*: arXiv:0803.4487.

[87] *Fermi surface and strong coupling superconductivity in single crystal NdFeAsO1T xFxC*. Liu, T. Kondo, M. E. Tillman, R. Gordon, G. D. Samolyuk, Y. Lee, C. Martin, J. L.McChesney, S.Bud'ko, M. A. Tanatar, E. Rotenberg, P. C. Caneld, R. Prozorov, B. N .Harmon, and A. Kaminski: *Fermi surface and strong coupling superconductivity in singlecrystal $NdFeAsO_{1-x}F_x$* arXiv: 0806.2147

[88] Lin Zhao1, Haiyun Liu1, Wentao Zhang1, Jianqiao Meng1, Xiaowen Jia1, GuodongLiu1, Xiaoli Dong1, G. F. Chen, J. L. Luo, N. L. Wang, W. Lu, Guiling Wang, YongZhou, Yong Zhu, Xiaoyang Wang, Zuyan Xu, Chuangtian Chen, and X. J. *Multiple NodelessSuperconducting Gaps in $(Ba_{0.6}K_{0.4})Fe_2As_2$ Superconductor from Angle-ResolvedPhotoemission Spectroscopy* :arXiv:0807.0398v2

[89] H. Ding, P. Richard, K. Nakayama, T. Sugawara, T. Arakane, Y. Sekiba,A. Takayama, S. Souma, T. Sato, T. Takahashi, Z. Wang, X. Dai, Z. Fang,G. F. Chen1, J. L. Luo1, and N. L. Wang: *Observation of Fermi-surface-dependent nodelesssuperconducting gaps in $(Ba_{0.6}K_{0.4})Fe_2As_2$* arXiv: 0807.0419

[90] C. de la Cruz et al, Nature **453**, 899 (2008).

[91]C. de la Cruz, Q. Huang, J. W. Lynn, J. Li, W. Ratcliff II, J. L. Zarestky,H. A. Mook, G. F. Chen, J. L. Luo, N. L. Wang and P. Dai: Nature **453**(2008) .

[92]A. Koitzsch, D. Inosov, J. Fink, M. Knupfer, H. Eschrig, S. V. Borisenko,G. Behr, A. K hler, J. Werner, B. B chner, R. Follath, and H. A. D rr:ouuPhys. Rev. B **78** (2008) .

[93]V. Vildosola, L. Pourovskii, R. Arita, S. Biermann, and A. Georges: Phys.Rev. B **78** (2008) .

[94] Myung,J.Han,Warren,E.Pickett,and Sergey,Y.Savrasov; Anist.*Itra.Magnetic frastration in high T_c I.Pnictides* (2009)

[95]I.I.Mazin,D.J.Singh,M.D.Johannes and M.H.Du *unconventional SC sighn reversal OP of* $LaFeAsO_{1-x}F_x$ (2009)

Declaration

This project is my original work, has not been presented for a degree in any other University and that all the sources of material used for the project have been dully acknowledged.

Name: shewangizaw hamelo

Signature:

Place and time of submission: Addis Ababa University, June 2011

.....

This project has been submitted for examination with my approval as University advisor.

Name: Prof. P.Singh

Signature: